Geological Quarterly, 2001, **45** (3): 229–255

Mineralogy of the Baszkówka chondrite (L5 S1): new data on silicates, opaques and minor minerals

Jerzy BORUCKI and Marian STĘPNIEWSKI

Borucki J. and Stępniewski M. (2001) — Mineralogy of the Baszkówka chondrite (L5 S1): new data on silicates, opaques and minor minerals. Geol. Quart., **45** (3): 229–255. Warszawa.

The mineral composition of the Baszkówka meteorite comprises: olivine, pyroxenes, plagioclase, Fe,Ni metal, troilite and chromite with minor chlorapatite, whitlockite, magnetite, haematite, spinel, idaite, calcite and native Cu. A rare variety of spinel (picotite), probably the oldest among the minerals of Baszkówka, was identified in the only two chondrules named: panda and chevron. The composition of the olivine (Fa 26.2±1.8 wt.%) and the high degree of chondrite homogenisation, a result of thermal metamorphism, are consistent with earlier results and indicate the L5 group. No distinct shock effects were observed in Baszkówka, classified as S1. Troilite-Fe,Ni and Fe,Ni metal lumps are defined and interpreted as molten planetesimals impact splashes.

Jerzy Borucki, Peszteńska 3 m 24, PL-03-925 Warszawa, Poland; Marian Stępniewski, Polish Geological Institute, Rakowiecka 4, PL-00-975 Warszawa, Poland (received: November 21, 2000; accepted: May 14, 2001).

Key words: Baszkówka, meteorites, ordinary chondrites, minerals, spinel (picotite).

INTRODUCTION

Meteorites have a relatively resctricted mineralogy relative to the Earth. The chondrite parent bodies were small, water-poor, devoid of oxygen, and the geological differentiation of primary matter is limited and scarce. In 1885 Gustav Tschermak gave a list of eighteen meteoritic minerals including four absent from the Earth (*fide* Manecki, 1971). In the last century, the number of the minerals found in meteorites grew slowly to ~20 species in 1950, and than to ~100 in 1970. Modern mineralogical methods, and new meteorite finds particularly on Antarctic ice and in Australian, American and African deserts, enabled further discoveries of meteoritic minerals. Rubin (1997) published a list of 275 extraterrestrial minerals (~10% of the Earth's total), including some present only as single grains in individual meteorites. Almost all of the main components of stony meteorites such as olivine, pyroxenes, and plagioclase are common in terrestrial rocks. But, the extraterrestrial environment is so different that of the Earth, that meteorites include rare exotic minerals such as carbides, silicides and nitride (e.g., Andersen *et al*., 1964; Wasson and Wai, 1970; Keil *et al.*, 1982; Alexander *et al*., 1991, 1994). Such minerals are absent from "normal" terrestrial environment, but are sometimes found in artefacts (Stępniewski and Borucki, 2001). Understanding the composition of meteorites is not simply a theoretical pursuit, but helps our understanding of the origin, development and the structure of the Solar System and of the Earth itself (Urey, 1952; Ringwood, 1966).

The inner part of the Baszkówka meteorite resembles a lithoclastic, coarse-grained sandstone with loosely packed "clastic" grains and a meagre, fine-grained, silicate matrix. The main clastic fraction is composed of globular, subglobular or ellipsoidal chondrules (from ~0.04 to ~3 mm in diameter), some as fragments (Siemiątkowski, 2001). Some chondrules are covered with condensation or accretion rims. Numerous, mostly intergranular voids are typical, though some cavities occur inside certain of the larger chondrules (Wlotzka and Otto, 2001). The low density (2.93 g/cm^3) of the chondrite (Stępniewski *et al*., 1998*b*) correlates with a high porosity ~18% on the Britt and Consolmagno diagram (Britt and Consolmagno, 1996; Consolmagno and Britt, 1996; Consolmagno *et al*., 1998), and matches the 20% porosity estimated by planimetric measurements (Siemiątkowski, 1998). Grains of Fe,Ni metal and troilite are scattered, mostly in the matrix, locally within chondrule rims, or dispersed as small blebs inside some chondrules. Most of the metal grains in the matrix have irregular contours, closely-fitted to the edges of the bordering silicates. A few rare metal or metal-troilite lumps (Stępniewski *et al*., 1998*a*) are present in the matrix. Numer-

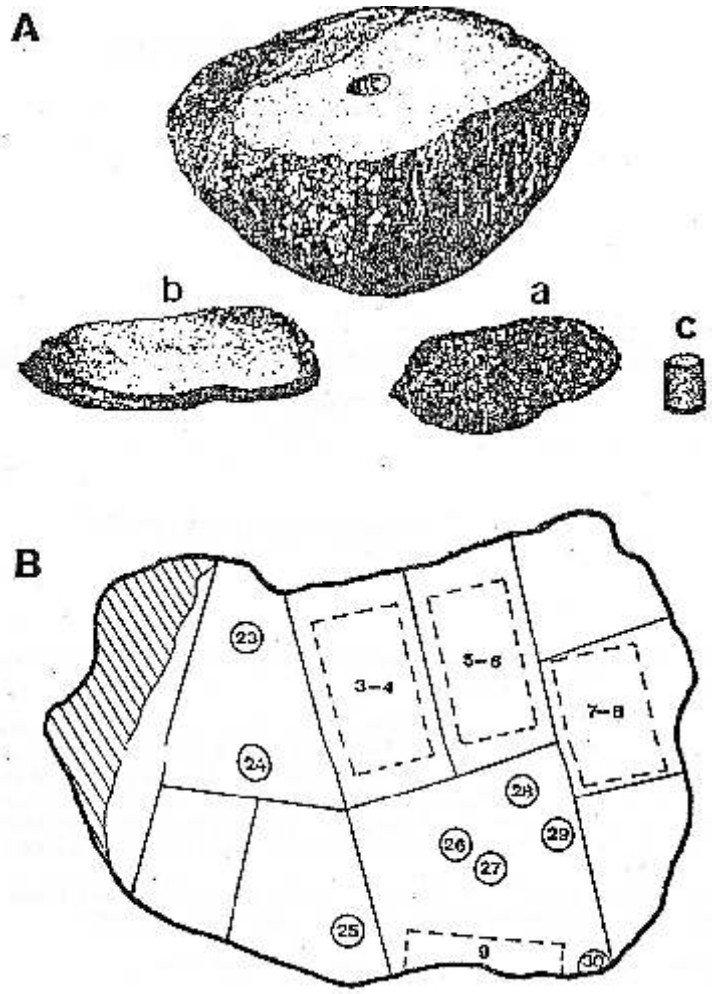

Fig. 1. Sampling scheme for the Baszkówka chondrite

A — two parallel cuts have dissected: a — a heel for collection and exchange, b — a plate for laboratory examination, c — cylinder from the interior of the stone was assigned to chemical analyses; **B** — the plate was divided into samples for thin sections (single numerals), and polished specimens for electron microscopy (double numerals)

Fig. 2. Baszkówka meteorite — the external surface of plate b from Fig. 1A; at left — a large metal-troilite particle, and a long chain of metal grains; at right, next to a fracture — four small metal-troilite particle; scale bar 20 mm

Fig. 3. Baszkówka meteorite — part of plate b from Fig. 1A; dark gray, globular or elliptical chondrules abound; some of them have the internal voids; shapeless light gray grains of metal, and brown-yellow grains of troilite are less frequent; at left — a metal-troilite particle, the largest one noticed in Baszkówka; the metal shell is partially split off; another smaller particle is visible at bottom right (arrow); below the particle a fragment of the metal chain is visible; scale bar 10 mm

Table 1

Chemical composition of olivine (in wt.%)

Analytical number	Na	Mg	Al	Si	Ca	Ti	Cr	Mn	Fe	Ni	O*	Total	Fo	Fa
Phenocrysts — B92, B93, chondrule rims — BOP, B48														
B49	0.00	22.55	nd	18.42	0.09	0.00	0.08	0.33	16.95	0.11	40.88	99.41	75.0	25.0
BOP	0.00	22.52	nd	17.88	0.09	0.00	0.00	0.36	17.19	0.00	40.17	98.21	74.6	25.4
B92	0.00	22.57	nd	17.99	0.13	0.03	0.08	0.18	17.68	0.00	40.51	99.17	74.6	25.4
B48	0.00	22.97	nd	17.81	0.04	0.00	0.00	0.43	18.08	0.00	40.65	99.98	74.0	26.0
B93	0.00	22.89	nd	17.99	0.02	0.04	0.00	0.47	17.64	0.02	40.12	98.19	73.5	26.5
Compound spinel chondrule: rim — B22, primary — B21, secondary — B20														
B22	0.29	21.10	0.06	18.79	1.00	0.11	0.00	0.44	17.41	nd	41.03	100.23	73.6	26.4
B21	0.00	21.49	0.41	18.91	0.15	0.14	0.67	0.31	17.57	0.00	41.40	101.05	73.5	26.5
B20	nd	22.46	0.00	18.64	0.00	0.03	0.24	0.29	18.88	0.00	41.19	101.73	72.9	27.1
Chondrite matrix														
B72	0.00	22.69	nd	17.74	0.00	0.00	0.02	0.31	17.56	0.24	40.33	98.89	74.5	25.5
B38	0.42	21.79	nd	17.90	0.10	0.00	0.00	0.58	18.35	0.00	40.39	99.53	72.5	27.5
Troilite-metal particle: silicate rim — B54, inclusions in kamacite — B55, B56														
B54	0.00	23.00	nd	18.18	0.06	0.07	0.12	0.20	17.77	0.00	41.08	100.48	74.8	25.2
B55	0.00	22.66	nd	18.42	0.04	0.06	0.11	0.34	17.57	0.00	41.13	100.33	74.4	25.6
B56	0.00	22.63	nd	18.45	0.01	0.00	0.00	0.41	18.01	0.00	41.07	100.58	73.8	26.2
Inclusions in kamacite particle														
B36	0.12	21.39	nd	18.78	0.02	0.04	0.09	0.47	18.09	0.00	40.72	99.72	72.6	27.4
B37	0.11	21.20	nd	18.48	0.06	0.00	0.00	0.47	18.44	0.00	40.19	98.95	72.0	28.0

nd— no data, * — stoichiometric; Fo — forsterite, Fa — fayalite

ous euhedral, mostly olivine, microcrystals appear in the voids (Wlotzka, 1997; Wlotzka and Otto, 2001).

This paper describes data from about a hundred mineralogical and chemical (electron microprobe — SEMQuant) analyses made in the laboratory of the Department of Petrology of the Polish Geological Institute during 1998–2000. Initial results were published in Stępniewski *et al*. (1998*a*) and Borucki and Stępniewski (2001).

SAMPLING AND METHODS

Cutting and sampling procedures were organised to avoid needless loss of material. The samples were representative, as far as possible, taking into the account the necessity of preserving most of the original shape of the stone. Some of the samples were localised and oriented.

The Baszkówka chondrite is a single, oriented stone shaped like a regular flat cone. Its surface is almost entirely (~93%) covered with an ablation crust, and sculptured with numerous, well developed, regmaglypts. Examination of the stone interior revealed a very porous structure, suggesting possible friability and a danger of damaging the specimen during sampling. Therefore, the specimen was initially photographed, described and a plaster casting was made. The sampling was started at the back surface of the stone, where the regmaglypts are absent and part of the ablation crust had broken off. Careful, slow, cold cutting of a heel and a slice was done with a diamond saw-blade disk 1 mm thick and 30 cm in diameter. A 25 mm diameter thin-walled hollow milling cutter was used to extract a sample from the inner part of the stone. The 50 mm thick heel was set apart for collections and exchange (Figs. 1Aa, 2 and 3), and a successive slice (~1 cm thick) was cut off for mineralogical, petrographic, and other physical and chemical studies

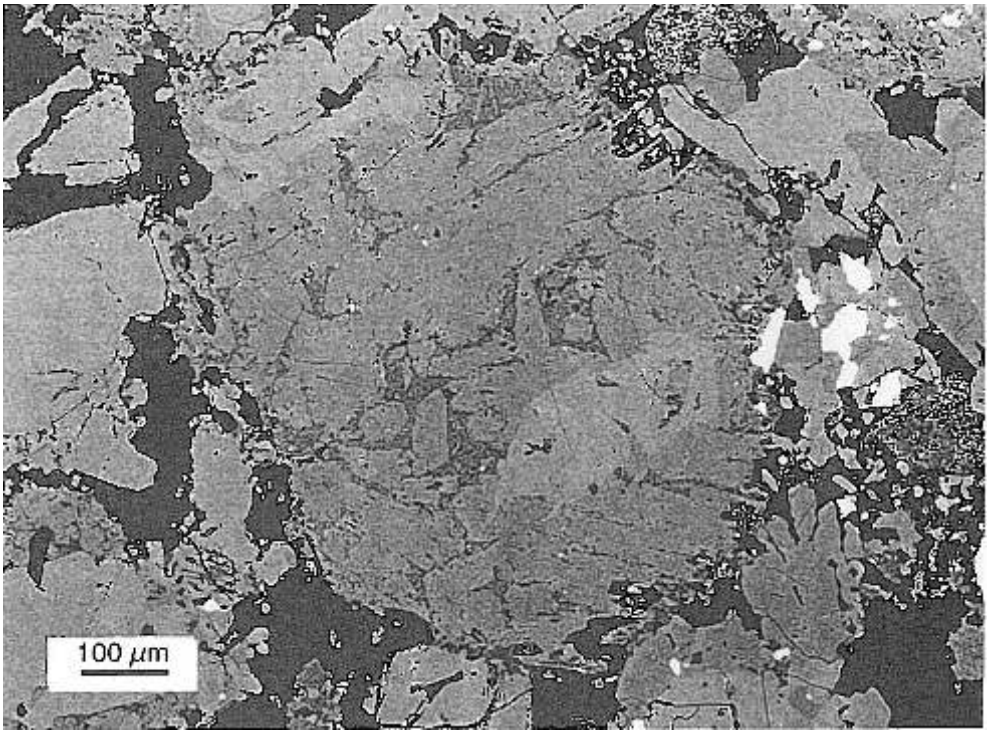

Fig. 4. BSE (backscattered electrons) image exposes a porphyritic chondrule with an olivine phenocryst (with euhedral pinacoid and pyramid faces), and dark gray, elongated, subhedral orthopyroxene phenocryst; dark gray mesostasis with scattered small metal blebs is composed mostly of symplectic aggregates of Ca-rich pyroxene and plagioclase

(Fig. 1Ab). The cylinder ~50 mm long, 25 mm in diameter (Fig. 1Ac) from the inside of the stone was appropriate for neutron activation analysis.

Thin sections for microscopic examination in transmitted light, and polished samples for reflected light and for electronic microprobe analysis were prepared using standard procedures. The agate mortars were used for manual preparation of analytical powders by grinding and homogenising, had been carefully cleaned with quartz powder and washed to minimize contamination. According to the analytical data (Dybczyński *et al*., 1999), the difficulties in grinding caused by the presence of the native iron do not bias the repeatability of the results. The sampling schema (Fig. 1B), showing the analytical destination of every specimen, allows correlation of the results with the various structures of the Baszkówka stone.

Quantitative chemical microanalyses were made with an Oxford electron microprobe and SEMQuant analytical program, for which the standard sample series were composed of minerals and/or artificial materials. Polarising microscopes made by *Ernst Leitz* (Wetzlar, Germany) and *MIN-8* (USSR) were used in mineralogical-petrologic studies, and the microscopic mineral identifications were supported by the X-ray EDS qualitative determinations.

RESULTS

The analytical result are outlined in ten tables and 25 attached photos, backscattered electron images (BSE) and scanning electron microscope images (SEM).

SILICATES

The study comprises analyses of olivine, orthopyroxene, Ca-rich pyroxene, and plagioclase, which are the main components of the chondrules and of the chondrite matrix, as well as of the inclusions enclosed inside the metal and metal-troilite particles.

Table 1 comprises 15 microprobe analyses of the different genetic and structural types of olivine:

1. Five analyses of phenocrysts from olivine PO and BO (porphyritic or barred) chondrules show a composition of olivine grains (Fig. 4), reflecting rapid (~1–10°C/h) crystallisation of a silicate melt in the temperature range 1200–1350°C (Weinbruch *et al*., 1996).

2. The next three analyses give the composition of a phenocryst and of an olivine grain from the rim of the spinel-bearing olivine chondrule panda (Borucki and Stępniewski, 2001), one of two unique chondrules found on the total surface area ~57 cm^2, of the thin sections analysed to date.

3. Two analyses of large olivine fragments represent the composition of a typical, abundant population of “clastic” olivine crystals, or their fragments. These are limpid, euhedral, short pinacoid crystals with pyramidal terminations. While most of the clastic olivines are homogenous, some display a zonal structure suggesting interrupted, two-fold crystallisation.

4. The next five analyses represent the composition of small, submillimetric subhedral olivine crystals enclosed in the troilite-Fe,Ni metal lumps (Fig. 5). Olivine crystals sealed in metal or in troilite have kept their euhedral crystal faces, but their edges are rounded as occurs on macroscale in pallasites in effect of annealing (Buseck, 1977; Scott, 1977).

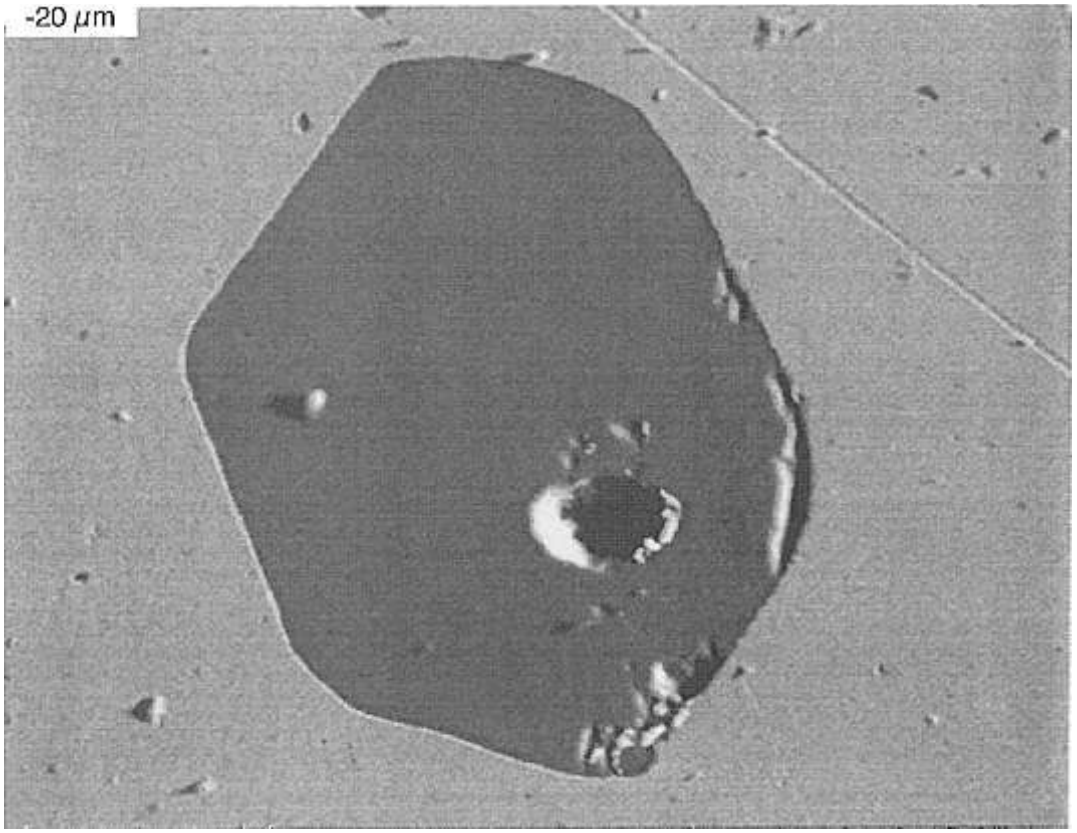

Fig. 5. BSE image; olivine crystal in Fe,Ni metal reveals euhedral pinacoid and pyramid faces; rounded edges show probable effects of annealing; the hole in the crystal remains after a probable fluid inclusion

The spectrometric procedures used in this study did not allow quantitative determinations on the surfaces of the submicrometric olivine crystals, present on the void walls (Fig. 6), as during the polishing of samples such crystals were spalled away. However, Wlotzka and Otto (2001), using more advanced techniques, have successfully analysed such crystals.

Orthopyroxene (OPX) is one of the main components of the radial pyroxene chondrules as well as in porphyritic pyroxene chondrules of the Baszkówka chondrite (Fig. 7). Together with olivine, OPX is the main component of porphyritic olivine-pyroxene and granular olivine-pyroxene chondrules. Notably, the structure of barred olivine-pyroxene (Fig. 8) chondrules comprises long, narrow laths, in each of which an olivine axis is bordered on both sides by an OPX lining, and the inter-lath spaces are filled with plagioclase. OPX "clastic" crystals and fragments are rare, but OPX inclusions in metal or metal-troilite particles are common. Eleven analyses of OPX are given in Table 2. Four of them are of phenocrysts, the next five represent the chemical composition of the OPX inclusions in the metal-troilite particles, and two last analyses are of the "clastic" OPX grains.

Ca-rich pyroxene (CPX) is exceptional among the components of Baszkówka in general. Nevertheless, CPX was recognised in the mesostasis of the porphyritic and barred chondrules, where it composes symplectite intergrowths with plagioclase (Fig. 9). The electron microprobe used in this study did not allow analysis of these tiny intergrowths, and only in few cases was it possible to get reasonable results (Table 3).

Plagioclase is not very abundant in Baszkówka, but its composition (Table 4) and structures are greatly diversified. The most frequent forms of plagioclase, easily discernible under the polarisation microscope in the matrix of the chondrite, are limpid oligoclase aggregates (<100 µm) with olivine, kamacite, and exceptionally CPXs or whitlockite. The SEMQuant analyses (B96, B43, B78 and B77) show low An,

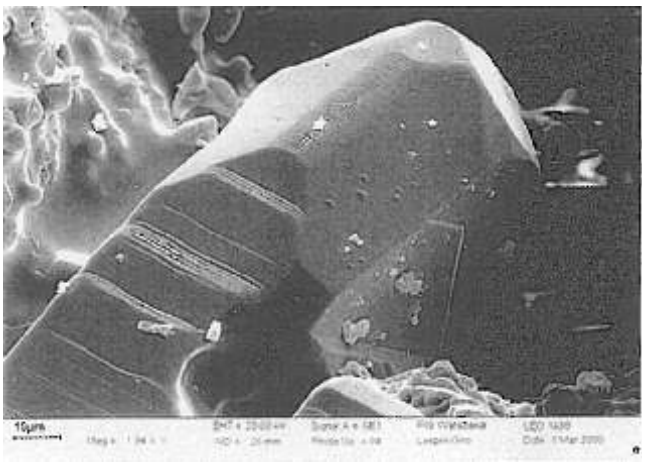

Fig. 6. SEM image; euhedral olivine crystal grown on a wall of an intergranular void; striated faces (growth accessories) suggest intermittent crystallisation

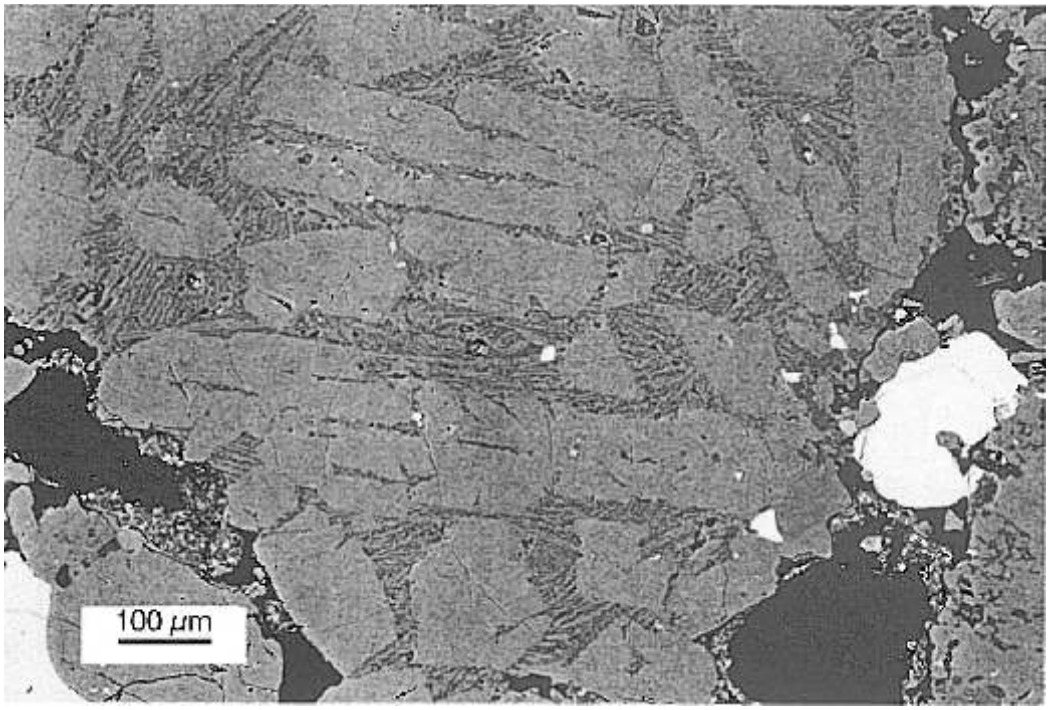

Fig. 7. BSE image; a porphyritic chondrule (without a rim) composed of elongated orthopyroxene phenocrysts and symplectic mesostasis (light gray, fine-grained clinopyroxene microlites intergrown with dark gray plagioclase); a grain of Fe,Ni metal in the matrix is discernible as a white-gray speck (at the left side of the picture)

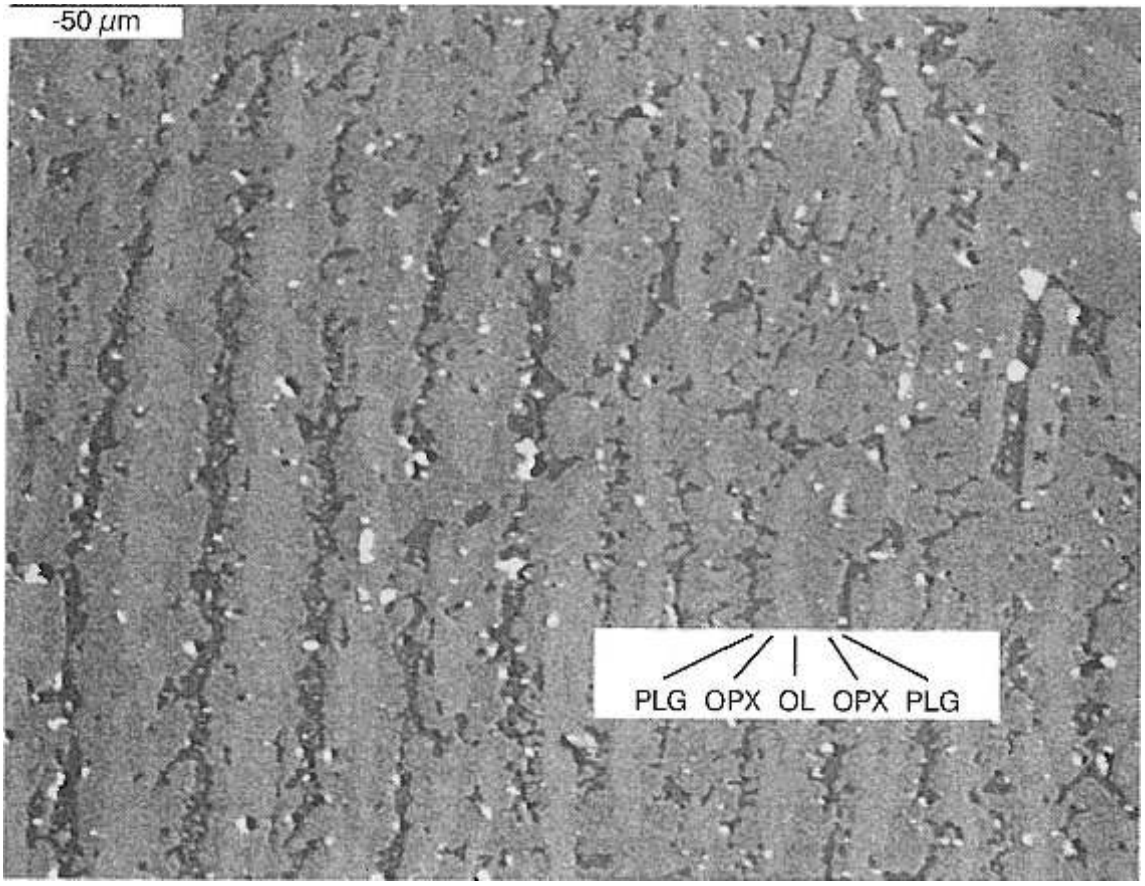

Fig. 8. BSE image; fragment of a chondrule with symmetrical bar structure, in which the central axis comprises light gray olivine (OL — Fa_{25}) with orthopyroxene (OPX — Fs_{22}) fringe on both sides, and dark gray plagioclase (PLG) mesostasis filling spaces between bars; numerous Fe,Ni metal blebs (white-gray patches) are dispersed in the silicates

Table 2

Chemical composition of orthopyroxene (in wt%)

Analytical number	Na	Mg	Al	Si	K	Ca	Ti	Cr	Mn	Fe	Ni	O*	Total	En	Fs	Wo
Chondrules: barred — B2522; porphyritic — B88, B82, B87																
B2522	nd	17.07	nd	26.67	nd	0.60	0.08	0.12	0.25	11.10	0.00	45.19	101.08	76.0	22.4	1.6
B88	0.26	17.20	0.14	26.23	0.00	0.69	0.05	0.00	0.41	10.61	0.00	44.76	100.35	77.3	20.8	1.9
B82	0.14	17.29	0.26	25.71	0.13	0.49	0.14	0.76	0.16	10.65	0.00	44.64	100.37	77.8	20.9	1.3
B87	0.01	18.07	0.01	26.20	0.08	0.45	0.14	0.16	0.42	10.46	0.00	45.10	101.10	78.9	19.9	1.2
Troilite-metal lump: inclusions in kamacite — B1109, B1042, B1133, B41, silicate rim — B39																
B1109	0.00	15.84	0.40	27.09	0.00	0.79	0.18	0.25	0.44	10.56	0.00	45.27	100.82	75.0	22.7	2.3
B39	0.00	16.02	0.20	27.20	0.00	0.69	0.02	0.12	0.17	11.31	0.00	45.15	100.88	75.0	23.0	2.0
B1042	0.00	16.07	0.25	27.22	0.00	0.71	0.03	0.30	0.04	11.11	0.00	45.29	101.02	75.2	22.8	2.0
B1133	0.13	16.58	0.00	26.19	0.00	0.81	0.13	0.06	0.29	11.19	0.00	44.35	99.73	75.5	22.2	2.3
B41	0.10	16.46	0.00	26.51	0.00	0.62	0.14	0.21	0.20	11.00	0.00	44.63	99.87	76.2	22.1	1.7
Chondrite matrix																
B73	nd	16.96	nd	26.63	nd	0.62	0.09	0.09	0.37	11.40	0.06	45.26	101.48	75.1	23.2	1.7
B40	0.18	16.54	0.06	25.69	0.08	0.68	0.20	0.01	0.17	11.29	0.00	43.85	98.75	75.6	22.5	1.9

En — enstatite, Fs — ferrosilite, Wo — wollastonite; other explanations see Table 1

from ~12 to ~22 wt.%, and Or from ≥3 to ≥6 wt.%. Plagioclase also forms symplectic structures with CPX in the mesostasis of the porphyritic and barred chondrules, easily visible on the BSE images (Figs. 8 and 9) but easy to overlook under the optical microscope, where they are visible only as small translucent dots. The corresponding SEMQuant analyses (Table 4, B97, B95, B94 and B91) show a composition of albite or oligoclase with variable contents of Or from ~3 to ≤6 wt.%. The B42 SEMQuant analysis of a plagioclase from the plagioclase-olivine-pyroxene inclusion in a metal particle shows a composition matching albite with Or >7 wt.%, as in the plagioclase of the chondrule mesostasis, but its size and shape is akin to the matrix plagioclase.

Plagioclase laths from the mesostasis of the spinel chondrule panda (Borucki and Stępniewski, 2001) show a trachitic-radiolitic texture, absent from other chondrules of Baszkówka. Moreover, the SEMQuant analyses point mostly to labrador (B14, B13, B16, B04, B11, B09 and B15) with a variable composition and low potassium contents. However, some laths with elevated sodium and partly also potassium contents show a composition of oligoclase (B17) or andesine (B10 and B12), whereas those enriched in calcium belong to bytownite (B15 and B05). On the other hand, the plagioclase from the rim of panda (B07 and B08), as well as the thin contact layer between the primary and secondary of that chondrule (B06) show an oligoclase composition, common in Baszkówka plagioclases.

OPAQUES

Kamacite, taenite and troilite grains, abundant in Baszkówka, display some varied structures and textures, however the most common are the separate anhedral particles of kamacite, and in some measure also taenite. Less frequent are kamacite-troilite intergrowths and subhedral or anhedral troilite grains. The most abundant anhedral kamacite grains (~0.6–<0.002 mm) have edges moulding around the walls of the surrounding silicates (Figs. 2–4 and 7). Troilite crystals, unlike kamacite, locally preserve some euhedral faces (Figs. 10 and 11). Infrequent chondrules contain abundant small kamacite and/or troilite blebs. Other scarce chondrules possess accretion rims made of silicates, troilite and/or kamacite grains (Fig. 12). In general, opaques from equilibrated ordinary chondrites show mostly aberrant, and locally fragmented shapes (Urey and Mayeda, 1959). However, in the case of Baszkówka, crystalline forms occur (Fig. 11), in which troilite has preserved euhedral faces. A distant likeness to the pyrophanite bearing-grain from the Leedey chondrite (McCoy *et al.*, 1997) may suggest that the subhedral grains from Baszkówka may have crystallised from melten chondrite material. An abundant variety of kamacite and troilite grains comprises small (≈0.6–0.03 mm) globules or ovoids wedged in fractures or attached to the surfaces of hollows. The free, rounded surfaces of the kamacite globules always display the effects of corrosion, not seen on the surfaces of troilite globules.

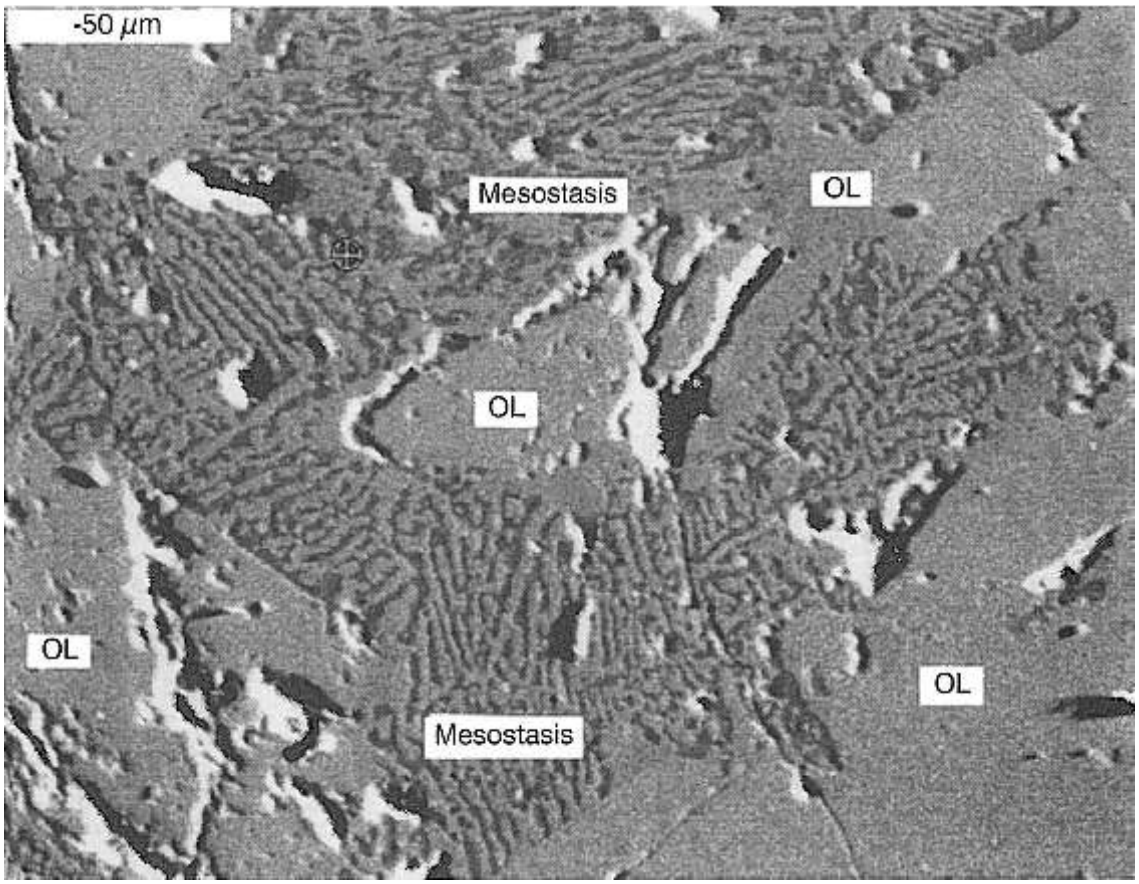

Fig. 9. BSE image; fragment of a chondrule with large, gray olivine phenocrysts (OL) and symplectic mesostasis composed of light gray clinopyroxene intergrown with dark gray plagioclase; the characteristic microporosity of the chondrule is visible

Troilite-kamacite (taenite) lumps (Figs. 13 and 14) rare in Baszkówka, and very rare in other ordinary chondrites. Most of these lumps, of which less than ten of are recognised to date, are up to >10 mm large (Figs. 2 and 3), and have concentric structures with large troilite cores covered with thin kamacite (taenite) shells. The outer rims are composed of small chon-

Table 3

Chemical composition of Ca-rich pyroxene (in wt.%)

Analytical number	Na	Mg	Al	Si	K	Ca	Ti	Cr	Mn	Fe	Ni	Zn	O*	Total	$Mg_2Si_2O_6$	$Fe_2Si_2O_6$	$Ca_2Si_2O_6$
B99	0.66	10.18	0.37	24.84	0.00	15.55	0.28	0.45	0.24	3.57	nd	nd	43.23	99.37	49.7	7.1	43.2
B84	0.60	10.29	0.36	25.60	0.00	16.20	0.31	0.48	0.09	3.72	0.00	nd	44.43	102.08	48.8	7.3	43.9
B83	0.34	9.88	0.58	24.85	0.08	15.92	0.31	0.59	0.17	3.22	0.00	nd	43.20	99.14	48.1	6.6	45.3
B81	0.28	10.37	0.44	25.23	0.00	16.66	0.18	0.61	0.29	3.41	0.00	0.37	44.15	101.99	47.9	6.7	45.4
B85	0.30	9.30	0.16	24.71	0.00	16.18	0.21	0.36	0.15	3.82	0.01	nd	42.39	97.59	45.5	7.9	46.6
B02	0.36	8.76	0.85	24.90	nd	17.56	0.35	0.66	0.23	3.76	nd	nd	43.71	101.14	42.6	7.7	49.7
B01	0.37	8.77	0.85	24.90	0.00	17.57	0.35	0.66	0.23	3.79	0.00	nd	43.61	101.10	41.6	7.8	50.6

Chondrule rims: B99, B01; other explanations see Table 1

Table 4

Chemical composition of plagioclase (in wt.%)

Analytical number	Na	Mg	Al	Si	K	Ca	Ti	Cr	Mn	Fe	Ni	Zn	O	Total	Ab	An	Or
Chondrite matrix																	
B96	6.23	0.65	11.23	29.76	0.80	1.56	0.05	0.00	0.00	0.51	nd	nd	47.37	98.16	82.0	11.7	6.3
B43	5.21	0.78	10.15	28.61	0.71	3.37	0.23	2.18	0.00	2.00	0.15	nd	47.20	100.59	73.0	21.1	5.9
B78	4.05	2.75	9.15	19.88	0.30	1.97	0.51	8.82	0.15	7.21	0.09	0.33	41.47	96.68	75.6	21.1	3.3
B77	5.38	nd	11.90	30.26	0.40	2.82	nd	nd	0.09	0.42	nd	nd	48.29	99.56	74.4	22.4	3.2
Porphyritic olivine chondrules (PO), symplectic mesostasis																	
B97	5.94	1.27	10.07	28.44	0.64	3.38	0.10	0.08	0.01	0.93	nd	nd	46.12	96.98	88.8	5.5	5.7
B95	6.41	0.36	11.41	29.40	0.67	1.68	0.00	0.00	0.00	0.30	nd	nd	46.87	97.10	87.9	6.7	5.4
B94	6.39	0.36	11.41	29.40	0.67	1.68	0.00	0.00	0.00	0.30	nd	nd	46.86	97.07	87.8	6.8	5.4
B91	2.44	6.15	4.87	26.85	0.19	9.76	0.11	0.44	0.09	2.39	nd	nd	44.74	98.03	73.0	23.9	3.1
Inclusion in metal lump																	
B42	5.18	1.10	9.93	31.50	0.76	1.10	0.00	0.00	0.00	2.31	0.00	nd	48.43	100.31	82.8	10.0	7.2
Spinel chondrule panda, mesostasis																	
B17	4.24	0.47	11.23	26.51	0.50	3.09	0.60	4.67	0.00	3.05	0.24	nd	46.71	101.31	67.2	28.1	4.7
B10	3.71	0.00	12.39	26.60	0.39	5.52	1.82	0.00	0.22	1.28	0.00	nd	46.45	98.38	54.0	46.0	0.0
B12	3.98	0.00	13.88	27.17	0.00	6.26	0.00	0.00	0.00	0.86	0.47	nd	46.96	99.58	52.5	47.5	0.0
B14	3.64	0.00	13.89	26.32	0.00	6.78	0.28	0.40	0.00	0.27	0.00	nd	46.51	98.09	48.4	51.6	0.0
B13	3.70	0.40	15.00	25.80	0.07	7.24	1.32	0.08	0.09	1.26	0.00	nd	48.59	103.55	47.1	52.9	0.0
B16	5.16	0.32	11.69	27.13	0.45	4.13	0.57	1.24	0.00	1.66	0.18	nd	46.48	99.01	47.1	52.9	0.0
B04	3.60	0.00	14.25	25.46	0.46	8.10	0.39	0.27	0.03	0.13	0.00	nd	46.54	99.23	42.3	54.5	3.2
B11	2.84	0.22	14.14	25.98	0.48	7.23	0.32	0.02	0.17	0.80	0.32	nd	46.89	99.41	39.1	57.0	3.9
B09	2.93	0.00	14.33	24.30	0.00	7.26	2.20	0.00	0.00	2.10	0.21	nd	46.41	99.74	41.3	58.7	0.0
B15	1.41	0.12	17.65	23.29	0.00	12.50	0.13	0.00	0.02	0.00	0.26	nd	47.73	103.11	16.5	83.5	0.0
B05	1.21	0.00	16.99	23.61	0.02	13.25	0.09	0.13	0.00	0.03	0.05	nd	47.58	102.96	15.4	84.5	0.1
Panda: contact layer primary-secondary																	
B06	3.90	6.39	7.93	25.64	0.39	1.51	0.10	0.03	0.63	7.70	0.59	nd	45.13	99.94	78.1	17.4	4.5
Panda: chondrule rim																	
B07	5.92	0.22	10.73	30.35	0.92	1.16	0.13	0.04	0.08	0.27	0.19	nd	47.24	97.25	83.1	9.4	7.5
B08	6.12	0.33	11.07	30.17	0.88	1.32	0.13	0.00	0.16	0.36	0.00	nd	47.39	97.93	82.7	10.3	7.0

Ab — albite, An — anorthite, Or — orthoclase; other explanations see Table 1

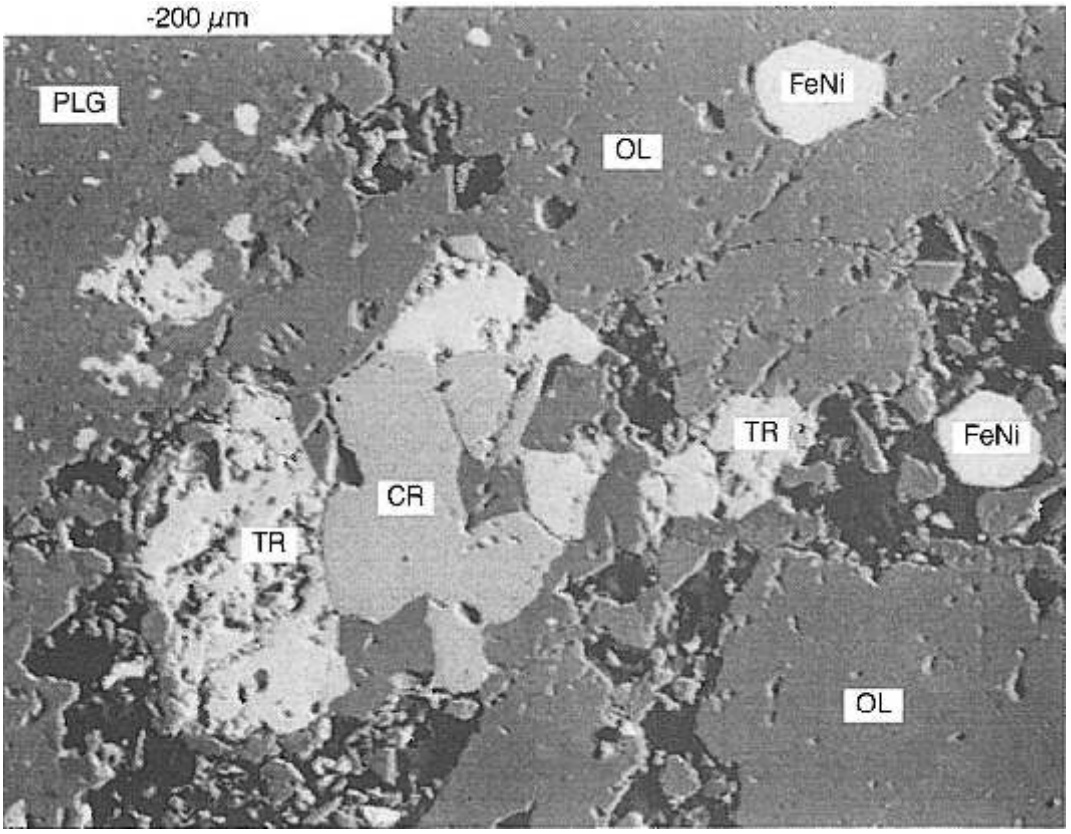

Fig. 10. BSE image; matrix of the Baszkówka chondrite: OL — dark gray, porous olivine grains; PLG — dark gray, composite plagioclase grains; CR — gray chromite grain intergrown with light gray, porous troilite (TR), and white-gray Fe,Ni metal (FeNi)

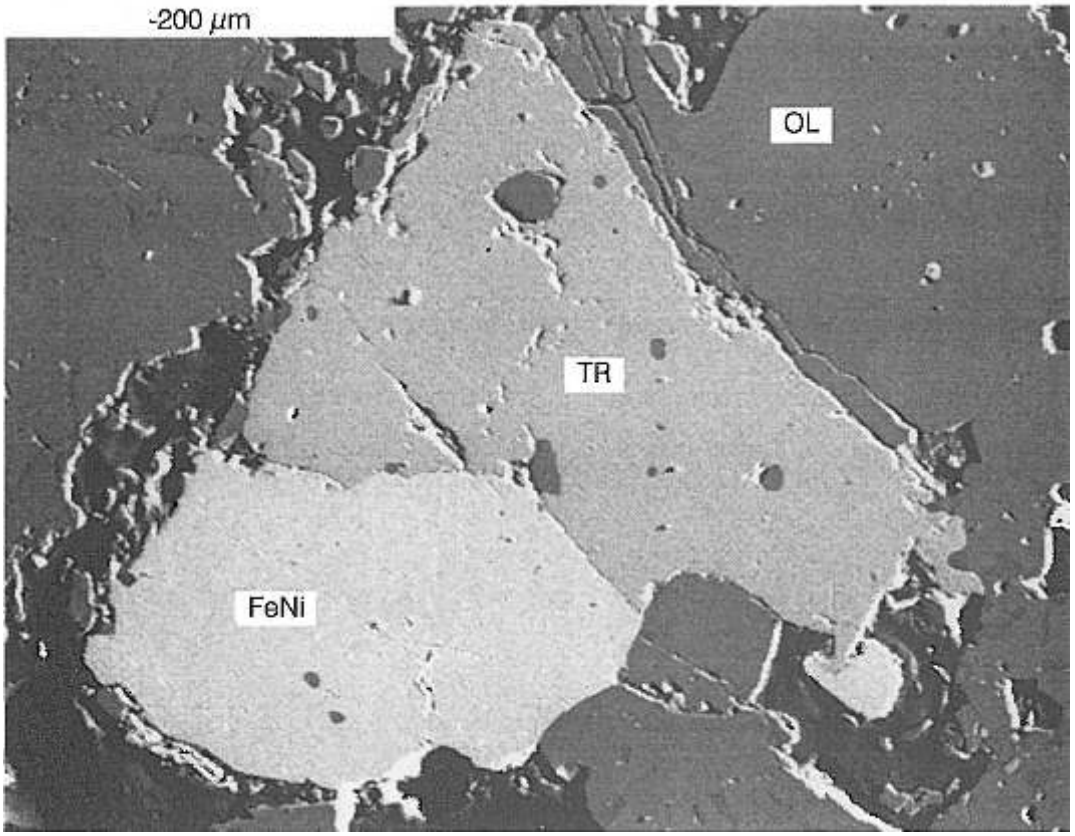

Fig. 11. BSE image; matrix of the Baszkówka chondrite: OL — olivine grains; TR — troilite, with euhedral basal pinacoid and pyramid faces, intergrown with Fe,Ni metal (FeNi)

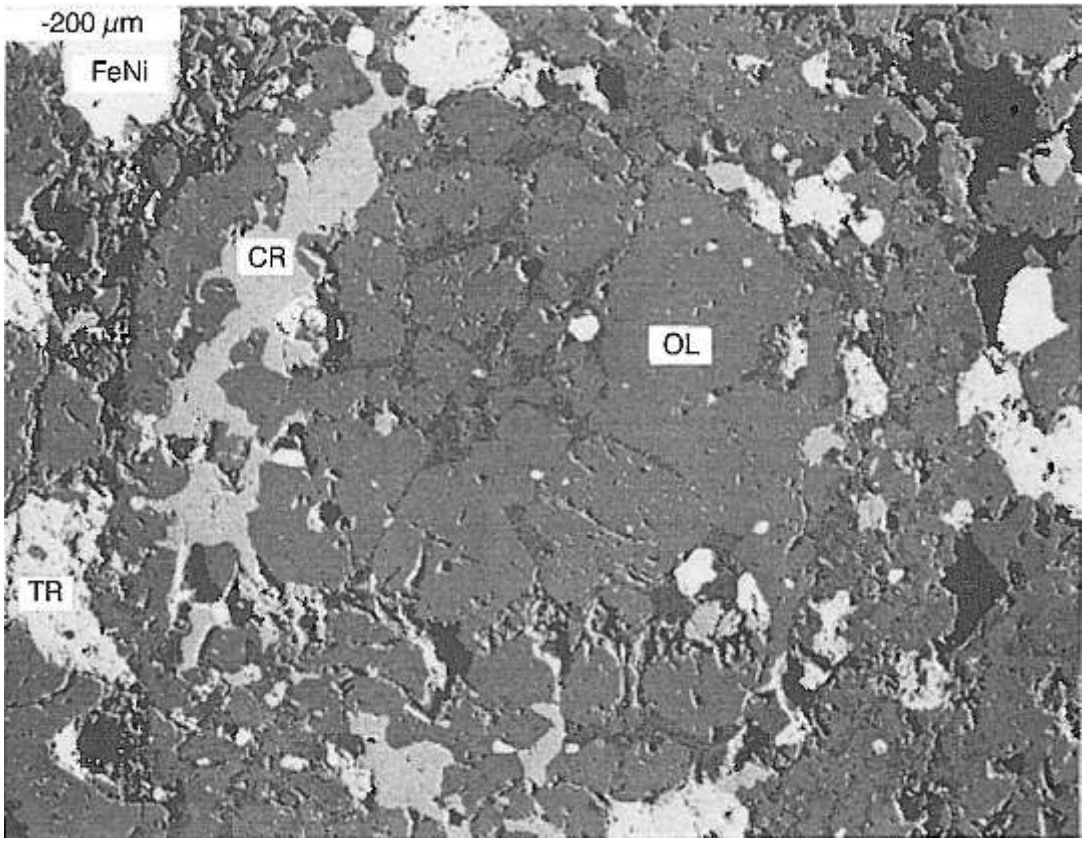

Fig. 12. BSE image; porphyritic olivine chondrule with a large rim; left part of rim: CR — gray, irregular, ameboid chromite grain intergrown with (dark gray) olivine (OL), and rare, small and porous (light gray) troilite (TR); matrix above the rim: FeNi — a grain of Fe,Ni metal; at the bottom: TR — troilite, to the right — an aggregate of troilite, olivine and plagioclase; a set of voids separates the chondrule from the matrix, except at the very bottom

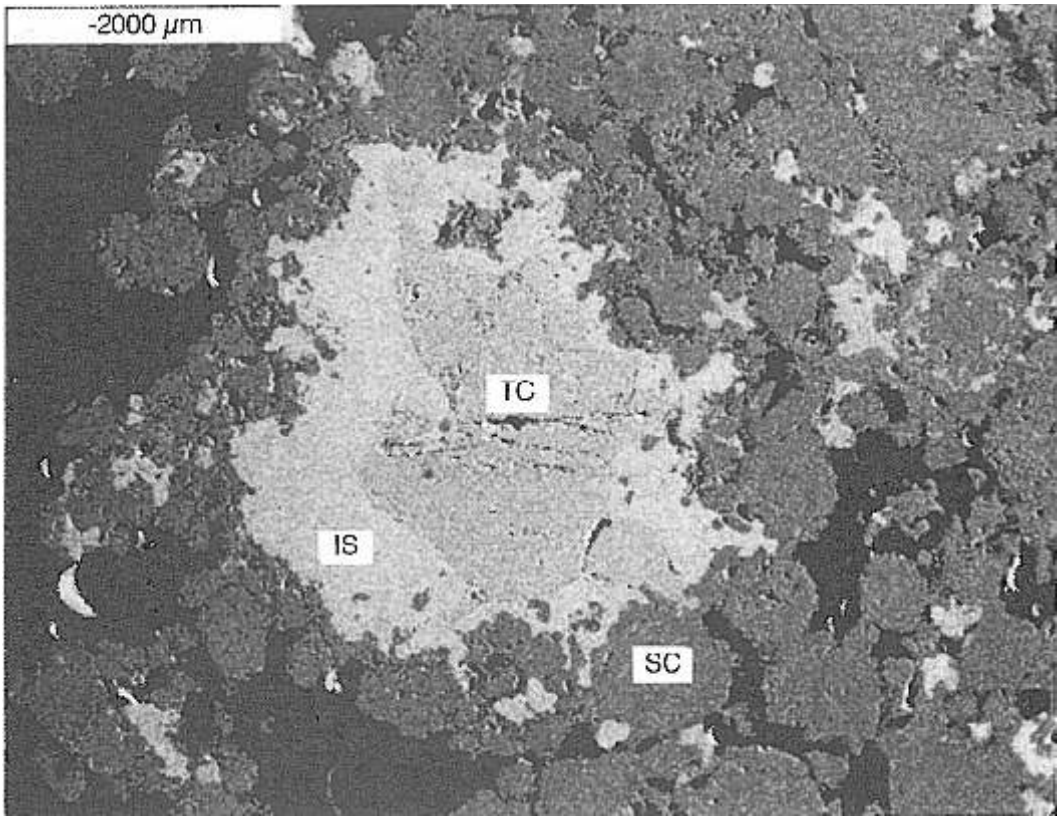

Fig. 13. BSE image; troilite-Fe,Ni (mostly kamacite) metal lump: TC — troilite core with smooth contact with IS — kamacite shell; sulphide and metal, most probably melted during deformation, have been deformed congruently; fractures in the core, absent from the shell, arose after the solidification, provoked by increasing differences between the deformability of troilite and kamacite; SC — silicate rim has a rough and jagged contact with the kamacite shell, rigid silicate grains having been forced into the molten metal; SC, composed of small chondrules, olivine and pyroxene grains, is separated from the chondrite matrix by a set of fissures

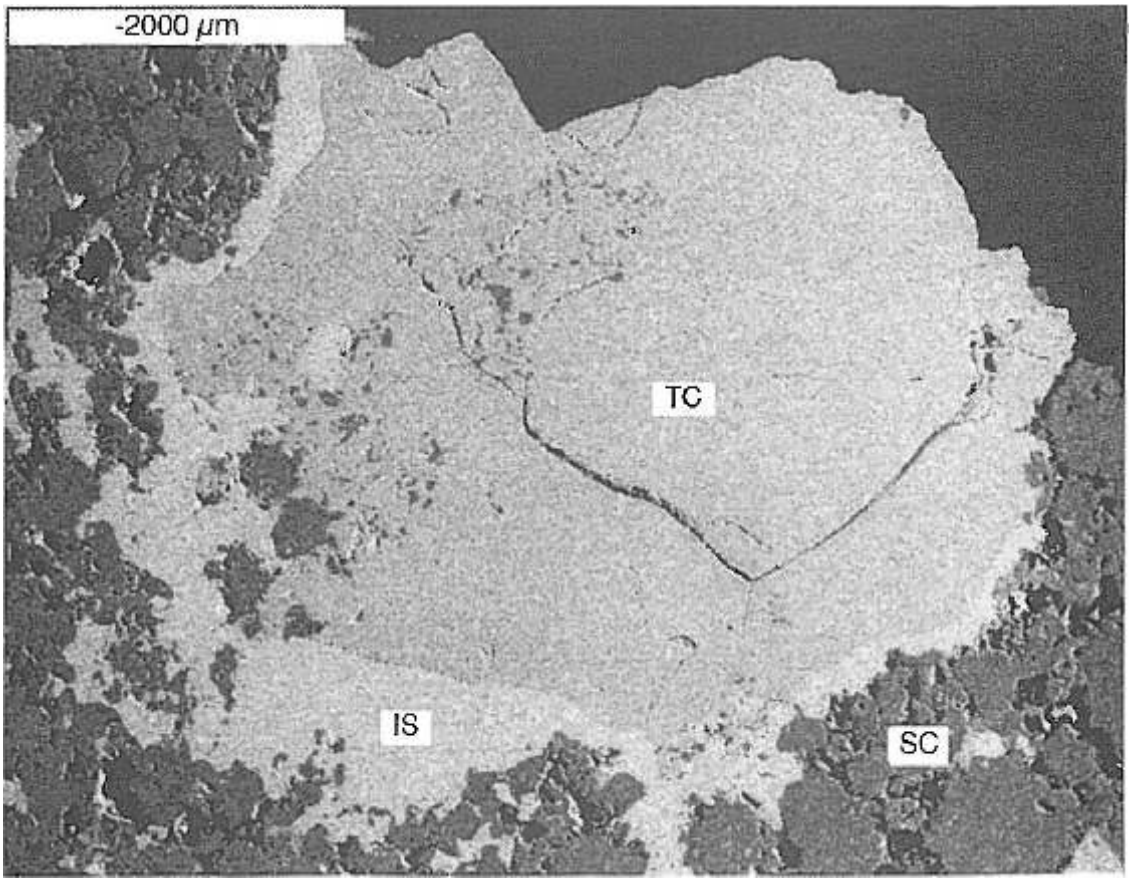

Fig. 14. BSE image; a fragment of the lump from (upper part destroyed during preparation): TC — troilite core with a few discernible fractures, IS — metal shell, SC — silicate rim; numerous silicate grains (dark gray spots) are visible at the left side of the lump

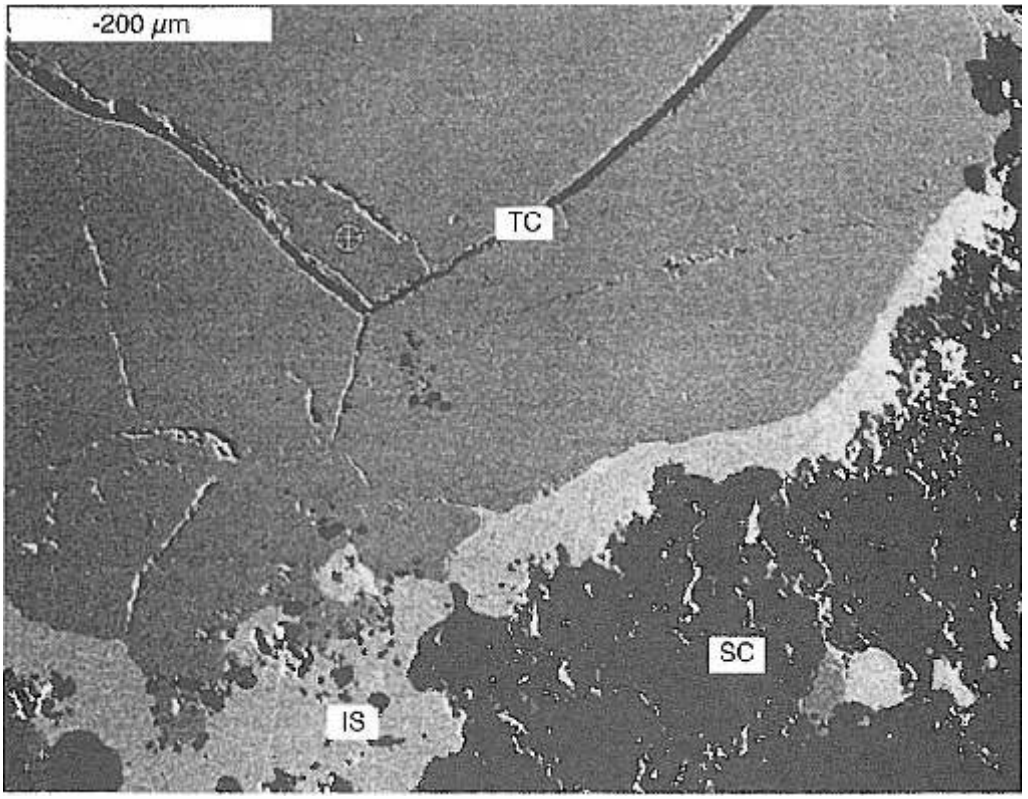

Fig. 15. BSE image; a fragment of the lump from Fig. 14: TC — troilite core with rare fractures and inclusions, IS — metal shell showing a smooth contact with core troilite and a rough and jagged contact with the silicate rim (SC); fractures are absent from the metal shell

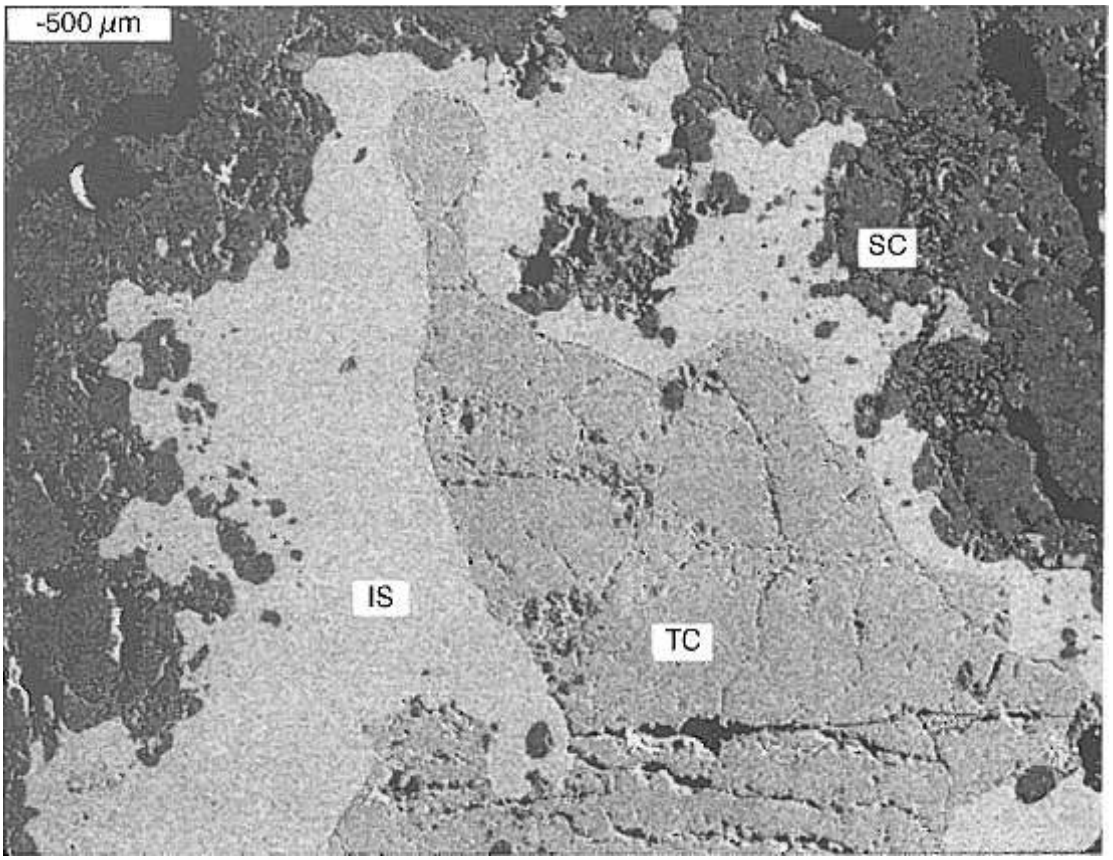

Fig. 16. BSE image; a fragment of the lump from Fig. 13: TC — troilite core with abundant irregular fractures stopping at the smooth contact with the metal, IS — metal shell showing rough, jagged contact with rim (SC), in which rigid silicate grains have been forced into the metal shells

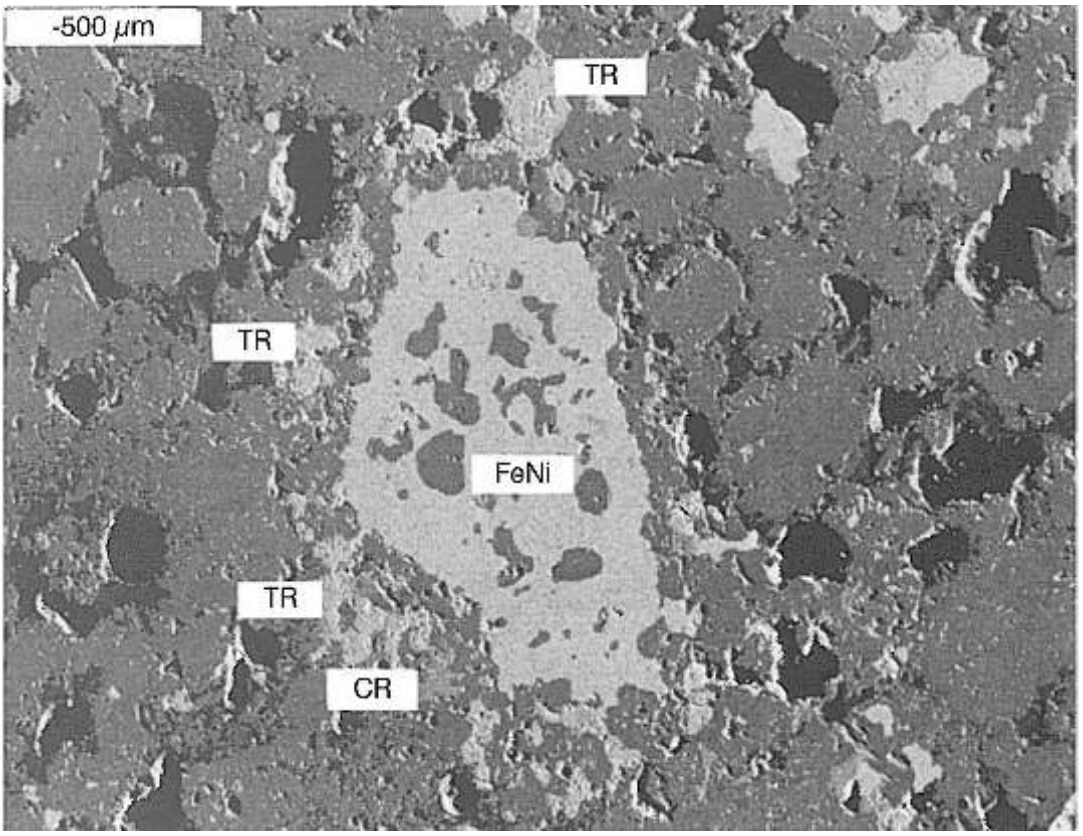

Fig. 17. BSE image; FeNi — a kamacite lump displays abundant inclusions of olivine, orthopyroxene, plagioclase and a grain of troilite; the rim of the lump, which is composed of smaller grains than the chondrite matrix, contains mostly olivine, pyroxene, troilite (TR) and few grains of chromite (CR); the metal-silicates contact is less uneven than in troilite-metal lump

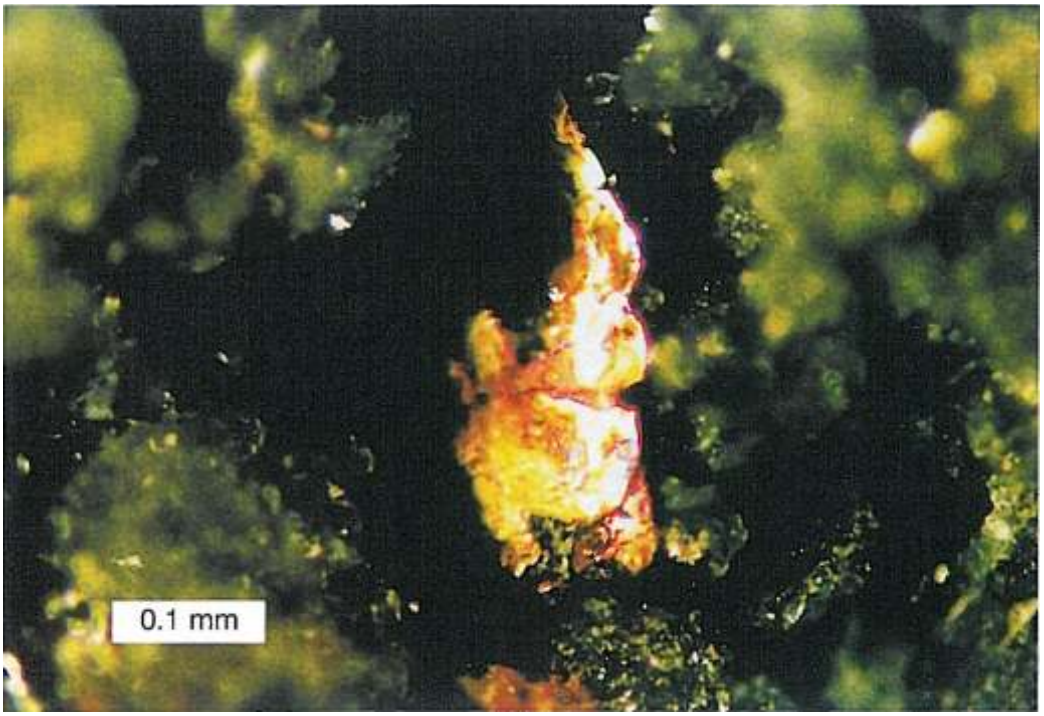

Fig. 18. Native copper grain found on a wall of cylinder c (Fig. 1A)

drules, olivine, pyroxene grains and/or fragments (Fig. 15). Contact of the silicate rim with the kamacite shell is rough and jagged because the contour of the shell is shaped by the rigid silicate grains forced into the easily molded Fe,Ni metal. The troilite core, tightly covered with the kamacite shell, only rarely contacts directly with the silicate rim, but where seen the metal-silicate contact is similar. The contact of the troilite core with the kamacite shell, conversely, is smooth, slightly undulose with sinus-like outlines (Fig. 16). Discontinuities occur between the outer rims of these composite particles (Fig. 13), cutting them off from the encircling material, suggesting that they are discrete entities accreted in the chondrite.

Some composite kamacite-troilite lumps comprise only kamacite cores and broken troilite rims, no silicate rims being observed.

Kamacite (taenite) lumps are rare but characteristic (Fig. 17) in Baszkówka. They are up to 4 mm long, have asymmetric shapes and undulose contours. They contain numerous inclusions of subhedral or anhedral olivine, pyroxene and rare troilite. The largest of the lumps is surrounded by an accretion rim, 50–100 mm wide, composed of olivine, pyroxene, troilite and a few grains of chromite. The smaller lumps have no discernible rim. Although the components of the rim are in general the same as in the chondrite, the proportions are different. The grains in the rim are smaller than those in the matrix, and there is an apparent prevalence of troilite and chromite. The rim contacts are lobed (but not as jagged as in the troilite-kamacite lumps) because of the numerous silicate grains pushed into the metal cores. In this way the rim grains are firmly fused with the metal cores forming together the discrete entities accreted in the chondrite. The lumps, at least the largest ones, are bounded by discontinuities (as with the troilite-kamacite particles) separating them from the rest of the chondrite material.

A few grains of native copper were found in the matrix of the Baszkówka chondrite. The largest, redish-orange copper lath (Fig. 18) was found inside the cylinder (Fig. 1Ac) taken from the center of the stone. The SEMQuant analyses from another thin layer of copper covering the surface of the contact between kamacite and troilite inside a metal-sulphide particle (Fig. 19) show contents of iron of 0.36–2.49 wt.% and nickel of 1.02–1.40 wt.% (Table 5).

CHROMITE AND SPINEL

Accessory **chromite** (Table 6) is scattered as separate grains or crystals in Baszkówka (Fig. 10). It is rare in the chondrule mesostasis and rims, or as a component of metal lumps rims (Fig. 17). Atoll textures, in which chains of small chromite grains encircle chondrules, are rare but distinctive (Manecki, 1972; Stępniewski *et al*., 1998*b*). More typical in Baszkówka are small, euhedral chromite crystals grown on the walls of voids and fractures in the matrix of the chondrite. Large crystal faces (Fig. 20) are possess abundant etch marks whose symmetry coincides the internal crystal structure. Their sharp edges preclude any dissolution following formation.

SEMQuant analyses of **spinel** (Fe, Mg-Al, Cr- picotite) are shown in Table 7. Some euhedral and subhedral picotite crystals are sealed in the plagioclase matrix in the panda chondrule. Another picotite skeletal crystal makes up the primary component of the chevron chondrule (Borucki and Stępniewski, 2001). The isotope composition of panda's picotite oxygen is different to that of chevron (Maruyama, 2001), suggesting their independent origin, though, petrological similarities hint at a genetic relationship between these chondrules.

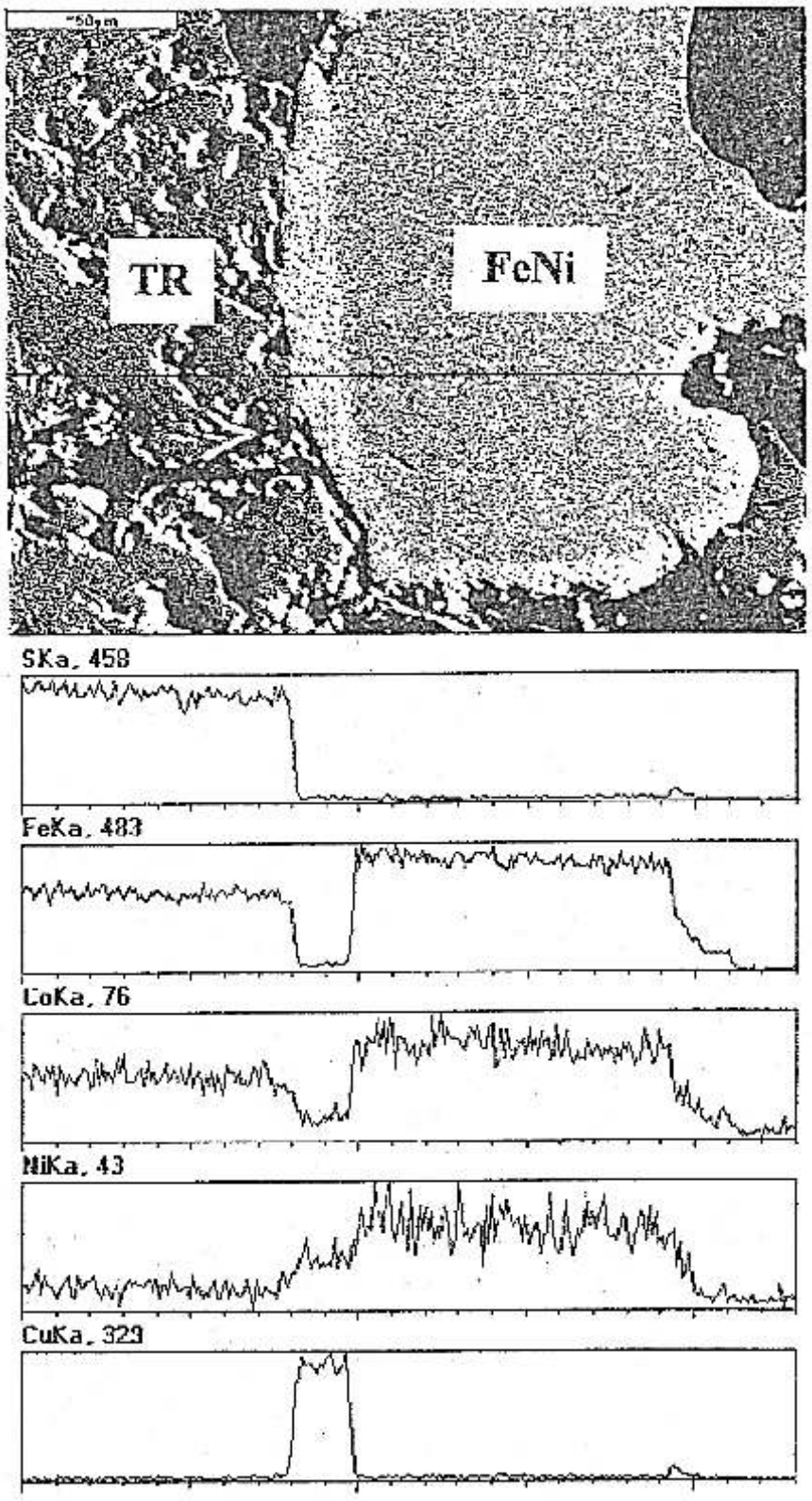

Fig. 19. BSE image; top— thin layer of native copper (white-gray) covering the contact between kamacite (FeNi) and troilite (TR); line indicates the spectral profile; bottom — scanning content of S, Fe, Co, Ni and Cu (excitation with an electron microbeam); the distribution of Cu suggests separation by diffusion

MAGNETITE AND HAEMATITE

Dusty **magnetite**, analysed only in two spots (Table 8), makes up the weathered microbreccia matrix which fills the spaces between the jagged kamacite fragments (Fig. 21). The magnetite microbreccia is the main element of the alteration zones generated by oxidation of Fe,Ni metal at surfaces of the troilite-metal particles. The SEMQuant analysis B51, in which

Table 5

Chemical composition of opaque minerals (in wt.%)

Analytical number	Mg	Si	S	Cr	Fe	Co	Ni	Cu	Zn	Total	Minerals
Troilite-metal particles: troilite core — B67, B69, B62; metal shell — B70, B68, B66, B58; silicate rim — B60; inclusion in kamacite											
B69	0.00	0.22	–	0.00	0.36	0.00	1.40	101.60	0.00	103.58	native cooper
B70	0.10	0.11	–	0.09	90.94	1.56	6.99	0.00	0.00	99.79	kamacite
B57	0.09	0.15	–	0.00	92.21	1.26	6.82	0.61	nd	101.14	
B58	0.01	0.19	–	0.02	91.08	1.46	6.20	1.90	nd	100.89	
B52	0.08	0.02	–	0.00	90.58	1.07	6.72	0.58	nd	99.05	
B68	0.00	0.10	–	0.06	44.14	0.60	55.75	0.65	0.00	101.30	taenite
B66	0.00	0.00	–	0.00	85.92	1.17	12.16	0.00	0.50	99.75	
B67	0.00	0.11	–	0.00	43.39	0.03	55.19	1.52	0.00	100.24	
B61	–	–	34.97	–	63.95	–	–	0.10	–	99.00	troilite
B62	–	–	35.26	–	63.47	–	–	0.40	–	99.13	
B60	–	–	35.13	–	63.82	–	0.00	0.23	–	99.18	
Metal particles											
B35	0.00	0.23	–	0.00	90.50	1.66	7.08	0.17	0.07	99.71	kamacite
B34	0.00	0.33	–	0.10	81.80	1.23	18.42	0.22	0.00	102.10	taenite
Metal and sulphide grains											
B74	0.14	0.01	–	0.05	71.82	1.19	26.08	0.28	0.00	99.57	taenite
B75	0.13	0.12	–	0.05	50.02	0.48	46.31	2.94	0.00	100.05	
B59	0.00	0.00	–	0.00	71.78	0.00	27.92	0.00	0.00	99.70	
B53	0.33	0.13	–	0.12	37.05	0.00	55.95	6.50	0.00	100.08	
B50	0.77	0.23	–	0.00	2.49	0.07	1.02	96.33	0.06	100.97	native cooper

Explanation see Table 1

oxygen was determined shows a significant excess of cations caused by incomplete oxidation of the Fe,Ni metal, which remains dispersed in the magnetite groundmass.

The presumed presence of haematite, a product of the further oxidation of Fe,Ni metal, was detected only on SEM images (Fig. 22). Small tablets growing on the surface of an olivine grain have well-developed basal pinacoid faces and triaxial symmetry, whereas X-ray EDS reveals almost exclusively the spectral lines of Fe and oxygen. Unfortunately, the probable haematite grains are to small and irregular for SEMQuant analysis.

PHOSPHATES

Four SEMQuant analyses of different whitlockite grains from the matrix of the Baszkówka chondrite are shown in Table 9. Whitlockite is an primary, extensive, accessory component of the matrix, reaching up to 0.1 mm large anhedral grains intergrown with olivine (Fig. 23). Between crossed polars whitlockite displays white-gray interference colours identical to plagioclase, but may be identified through its uniaxial conoscope image. In contrast to whitlockite, chlorapatite was noticed only at one spot on a SEM image (Fig. 24), in a void between olivine, plagioclase and troilite grains. The secondary origin of the isometric (<0.1 mm) euhedral crystals of chlorapatite contrast with the primary whitlockite.

SULPHIDES

We have outlined the troilite mode of occurrence below in the chapter on opaques in Baszkówka. The chemical composition of troilite (Table 5), taking into account small contents of

Table 6

Chemical composition of chromite (in wt. %)

Analytical number	Mg	Al	Ca	Ti	V	Cr	Mn	Fe	Zn	O*	Total
B44	1.52	2.69	–	2.02	–	39.23	–	24.58	–	29.89	99.93
B46	1.41	2.40	–	2.18	–	39.48	–	24.91	–	29.87	100.25
B47	1.50	2.77	–	1.95	–	38.72	–	24.53	–	29.65	99.12
B03	0.88	2.64	–	1.21	–	39.91	2.46	23.70	0.33	29.74	100.87
B33	1.13	2.43	0.29	1.97	0.29	38.32	1.77	23.98	0.28	29.66	100.02
B45	1.46	2.85	–	1.18	–	39.04	–	24.19	–	29.23	97.95
B79	1.47	3.21	–	2.21	–	38.82	–	24.82	0.20	30.37	101.10
B80	1.44	2.92	–	2.18	–	37.74	–	25.33	0.29	29.75	99.66
Cation formula based on 4 oxygen atoms											
Analytical number	Mg	Al	Ca	Ti	V	Cr	Mn	Fe	Zn	Mg+Fe+Mn	Al+Ti+Cr
B44	0.13	0.21	–	0.09	–	1.62	–	0.94	–	1.07	1.92
B79	0.13	0.25	–	0.10	–	1.57	–	0.94	0.01	1.07	1.92
B46	0.12	0.19	–	0.10	–	1.63	–	0.96	–	1.08	1.92
B47	0.13	0.22	–	0.09	–	1.61	–	0.95	–	1.08	1.92
B45	0.13	0.23	–	0.05	–	1.64	–	0.95	–	1.08	1.92
B03	0.08	0.21	–	0.05	–	1.65	0.10	0.91	0.01	1.09	1.91
B33	0.10	0.19	0.01	0.09	0.01	1.59	0.07	0.93	0.01	1.10	1.87
B80	0.13	0.23	–	0.10	–	1.56	–	0.98	0.01	1.11	1.89

Explanations see Table 1

copper, agrees with the theoretical proportion of sulphur and iron in the formula of FeS. Therefore the mean content of troilite in Baszkówka, calculated on the basis of X-ray diffraction analysis of a bulk sample (Rigaku Application Laboratory, 1997), assuming that all sulphur is contained within FeS (other sulphides being extremely rare), have given 5.8 wt.%. Two kinds of troilite were noticed — massive and porous — subsequent study being of their chemical composition or structural and textural relations. Besides troilite, only one other sulphide mineral — a possible idaite — was detected in Baszkówka (Fig. 24), qualitatively, on the basis of an X-ray EDS spectrum.

CARBONATES

The appearance of secondary calcite, the only carbonate found to date in Baszkówka, as a group of rhombohedral crystals arrayed in a "cauliflower" structure (Fig. 25), was inferred from an X-ray EDS spectrum with a strong Ca-line. Its origin is most probably related to limited terrestrial weathering.

DISCUSSION

Preliminary studies (Stępniewski *et al.*, 1998*a*) of Baszkówka suggested that it was distinctive among EOCs (equilibrated ordinary chondrites). Here, this distinctiveness is seen to be expressed in the relatively diverse mineral composition, comprising refractory (and possibly relict) picotite, abundant olivine, pyroxenes, plagioclases, kamacite, taenite and troilite, accessory chromite and whitlockite, together with secondary oxidation products such as magnetite, haematite, chlorapatite and calcite. Moreover, the diverse structures and textures observed in Baszkówka suggest a particular genetic significance.

DIVERSIFIED CHEMICAL COMPOSITION OF SILICATES

The mean content of fayalite in olivine is (Fa = 26.2±0.9 wt.%) analysed (n = 15) (Table 1), is not entirely representative

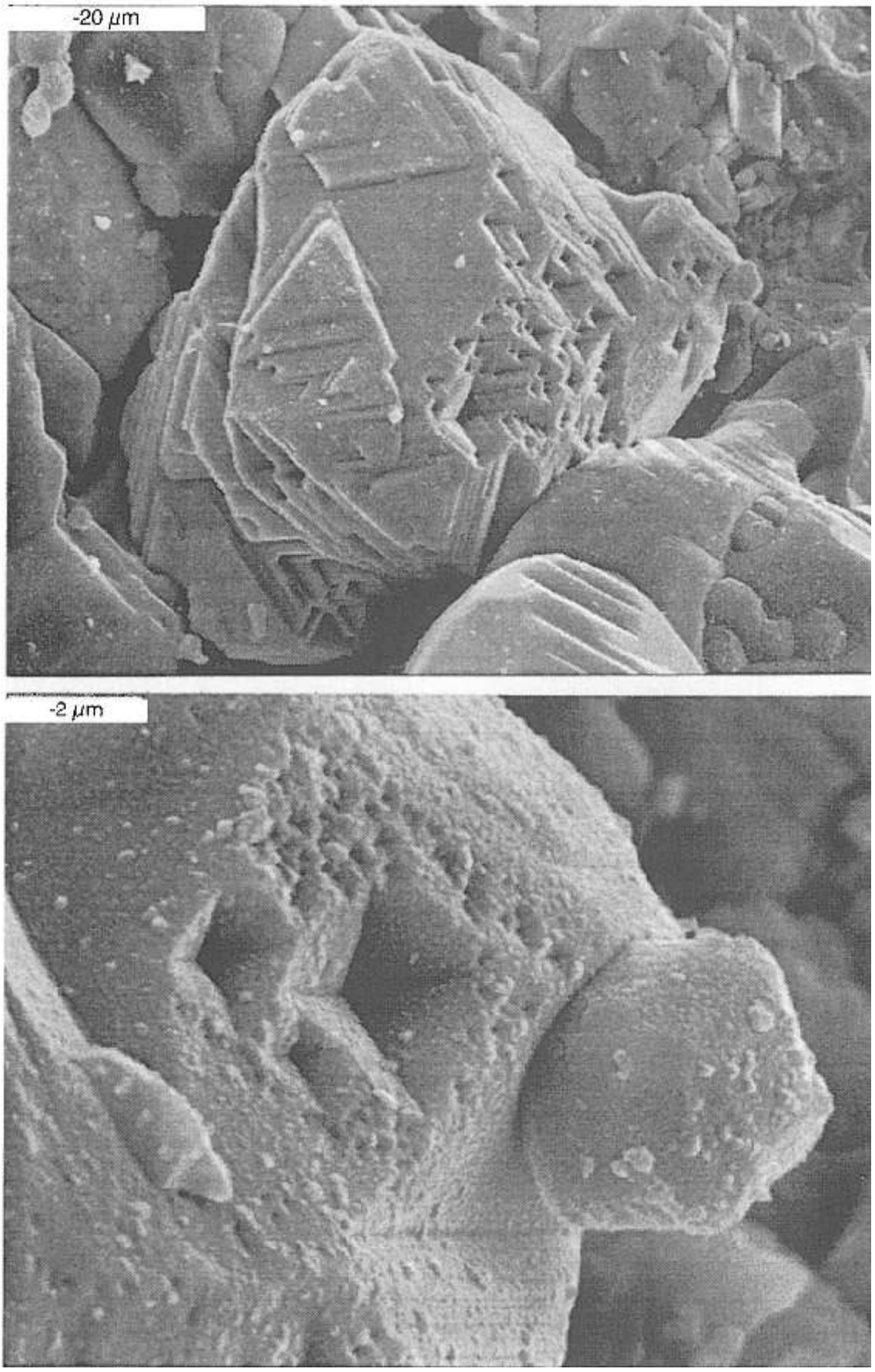

Fig. 20. SEM image; chondrite matrix: euhedral crystals of chromite in a fracture; the crystal walls are decorated with geometric etch figures displaying sharp corner

Table 7

Chemical composition of picotite (in wt.%)

Analytical number	Mg	Al	Ti	Cr	Mn	Fe	Zn	O	Total
B32	5.90	19.76	0.44	18.57	0.96	19.40	0.27	36.26*	101.59
B31	5.35	19.38	0.26	18.59	1.13	19.26	nd	37.22**	101.19
B30	5.35	19.39	0.26	18.56	1.13	19.25	nd	35.34*	99.28
B29	6.04	21.72	0.18	17.04	0.80	18.57	nd	36.84*	101.19
B28	6.04	21.72	0.18	17.05	0.80	18.58	nd	38.08**	102.45
B27	7.86	24.37	0.15	12.93	nd	15.92	0.82	37.68*	99.73
B26	7.87	24.37	0.15	12.95	nd	15.93	0.82	40.27**	102.36
B25	7.73	24.53	0.19	10.68	0.00	16.26	0.48	43.79**	103.66
B24	7.07	24.29	0.00	11.71	0.43	18.22	0.00	38.42**	100.14
B23	8.10	24.74	0.24	11.29	0.84	17.67	0.47	38.138	101.48
Cations formula based on 4 oxygen atoms									
Analytical number	Mg	Al	Ti	Cr	Mn	Fe	Zn	Mg+Fe	Al+Cr
B25	0.465	1.329	0.006	0.300	0.000	0.425	0.011	0.890	1.629
B26	0.515	1.435	0.005	0.396	0.000	0.453	0.056	0.968	1.831
B28	0.417	1.352	0.006	0.551	0.024	0.559	nd	0.977	1.903
B31	0.399	1.235	0.009	0.614	0.035	0.593	nd	0.992	1.850
B29	0.432	1.399	0.006	0.569	0.025	0.578	nd	1.009	1.968
B30	0.398	1.301	0.010	0.646	0.037	0.624	nd	1.022	1.947
B24	0.484	1.499	0.000	0.375	0.013	0.543	0.000	1.027	1.875
B27	0.549	1.534	0.006	0.422	0.000	0.484	0.021	1.033	1.957
B32	0.428	1.292	0.016	0.630	0.031	0.616	0.007	1.041	1.923
B23	0.560	1.539	0.008	0.365	0.025	0.531	0.012	1.090	1.904

* — calculated stoichiometrically, ** — analysed; other explanations see Table 1

Table 8

Magnetite cement from microbreccia in troilite-metal lumps oxidation zone (in wt.%)

Analytical number	Mg	Si	Ca	Fe	Co	Ni	O	Fe+Ni+Co+Mg+Si	Total
B51	0.180	0.240	0.070	70.080	0.700	2.370	22.020	–	95.66
B51*	0.021	0.024	0.005	3.647	0.035	0.118	4.000	3.800	–
B71	0.140	0.260	0.000	71.680	0.480	2.040	21.600	–	96.20
B71*	0.018	0.028	0.000	3.802	0.024	0.103	0.000	3.975	–

* Cations formula based on 4 oxygen atoms; oxygen in B51 sample determined by electron microprobe

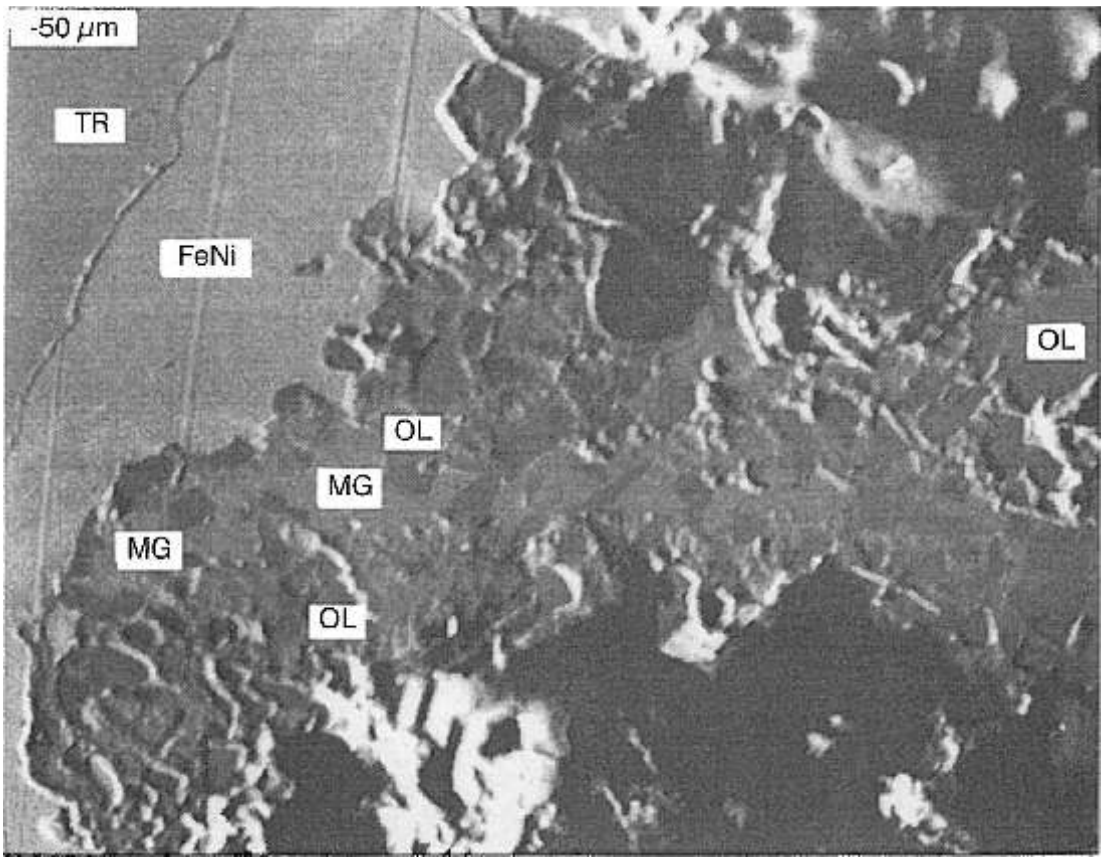

Fig. 21. BSE image; a part of the particle rim from Fig. 15: TR — troilite core, FeNi — metal shell, OL — olivine; olivine microbreccia with magnetite cement (MG)

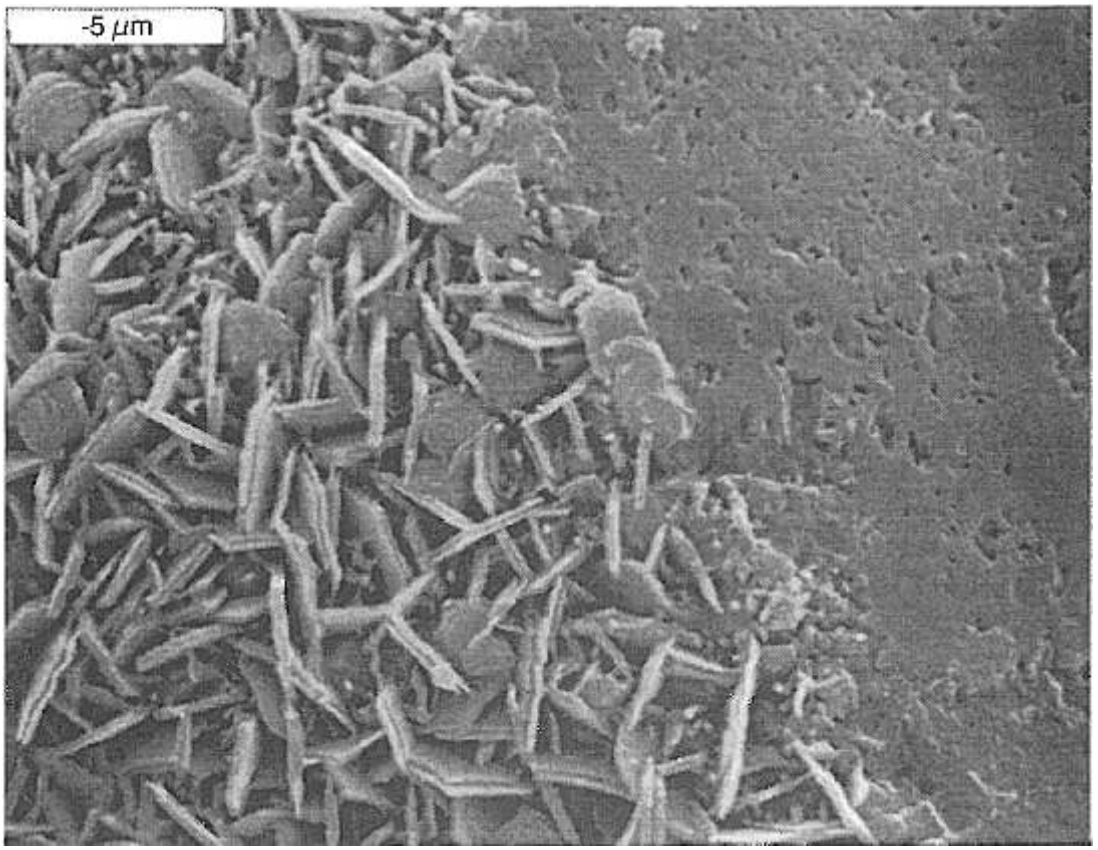

Fig. 22. SEM image; haematite crystals on the surface of an olivine grain

Table 9

Chemical composition of whitlockite (in wt. %)

Analytical number	Na	Mg	Al	P	Ca	Mn	Fe	O*	Total
B64	1.70	1.82	nd	20.98	32.68	nd	0.60	42.10	99.88
B63	1.87	1.66	nd	20.13	34.24	nd	0.00	41.38	99.28
B65	1.97	1.84	nd	21.05	33.15	nd	0.36	42.42	100.79
B76	1.69	1.67	0.10	20.20	33.84	0.09	0.76	41.61	99.96
Cations formula based on 8 oxygen atoms									
B64	0.23	0.23	–	2.06	2.48	–	0.03	8.00	–
B63	0.25	0.21	–	2.01	2.64	–	0.00	8.00	–
B65	0.26	0.23	–	2.05	2.50	–	0.02	8.00	–
B76	0.23	0.21	0.01	2.01	2.60	0.01	0.04	8.00	–

Explanations see Table 1

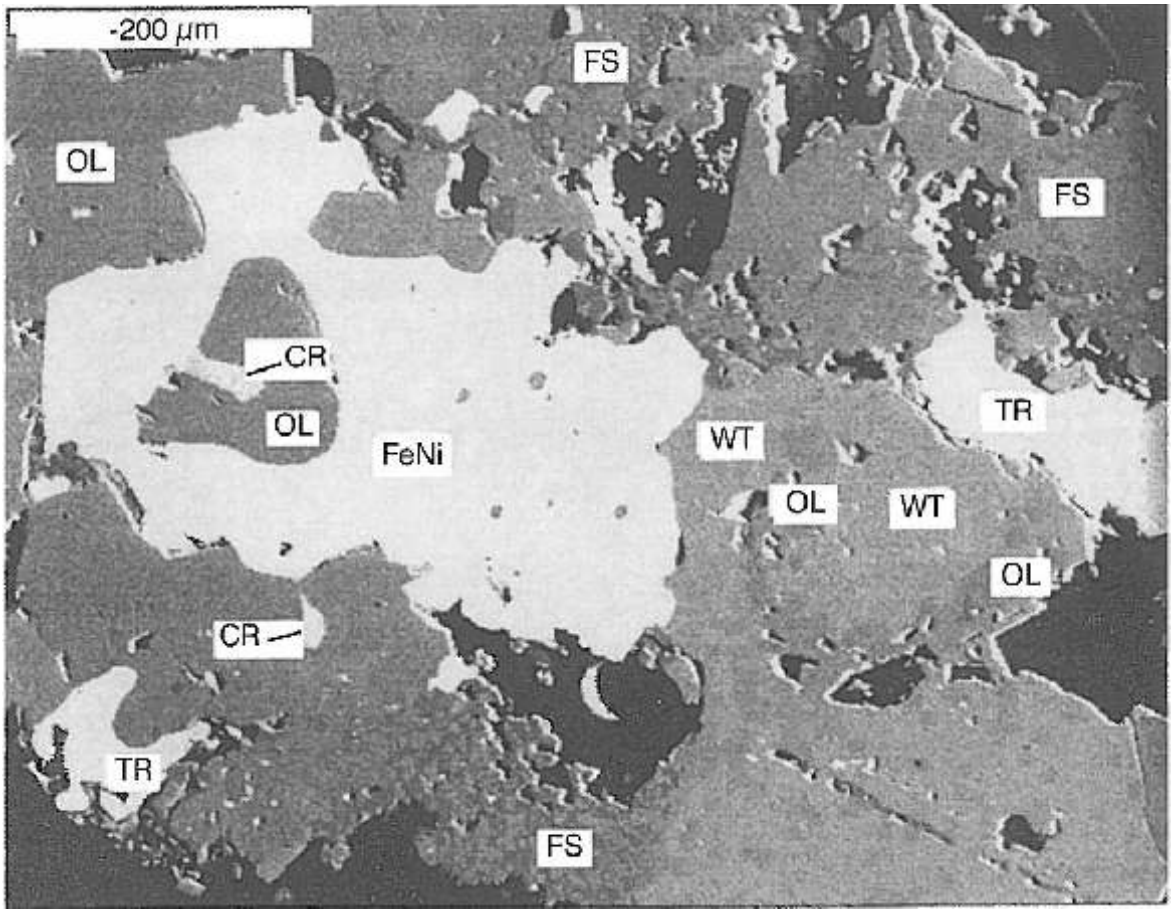

Fig. 23. BSE image; chondrite matrix reveals a complex intergrowth of submillimetric olivine (OL), troilite (TR), chromite (CR), and whitlockite (WT) grains; a metal grain (FeNi) border conforms to the contour of a subhedral olivine grain (OL); orthopyroxene occurs as microaggregates with plagioclase (FS)

Fig. 24. SEM image; euhedral crystals of chlorapatite in a fissure within chondrule matrix

for Baszkówka, since the selection of objects analysed was not random, as grains selected for analysis were chosen to characterise specific structures. Some occurrences were analysed more frequently (e.g., olivine from the spinel-bearing chondrules or olivine from the Fe,Ni metal particles) than if the selection would be indiscriminate. Analyses of the phenocrysts of the olivine chondrules and of clastic olivine grains are more representative of the body of the chondrite. A selective mean is Fa = 25.9±0.83 wt.% (n = 7), relative standard error ±3.2 wt.%. The difference between the two means is insignificant.

The average content of Fa in Baszkówka olivine (Table 10) is located between, and outside of both limits, for L and H chondrites as fixed by Rubin (1990). It is 0.7 wt.% below the minimum for H chondrites, but exceeds only by 0.1 wt.% the maximum for the L chondrites. Homogenisation of chondrites and ordering to petrologic type is mostly evaluated using structural/textural features, though also on the homogeneity of the chemical composition of olivine and pyroxenes, viz., FeO "per cent mean deviation" (Van Schmus and Wood, 1967). In consequence, the statistical characteristics calculated for Baszkówka (mean, $\bar{X}_{FeO}$ = 26.68 wt.% and standard error of mean = 0.2335 wt.%, or relative 1.03 wt.%) suggest significant homogenisation and consequently the high petrologic type L5, consistent with previous work (e.g., Wlotzka, 1995; Stępniewski *et al*., 1998*b*).

Low-Ca pyroxene in Baszkówka shows intense homogenisation. Contents of En, Fs and Wo (Table 2) in the pyroxene (low-Ca bronzite) grains reveal a small dispersion, in spite of the significant differences of structures they belong to. For instance, there is little chemical difference between pyroxene grains from genetically very different structures such as matrix and inclusions in a Fe,Ni metal particle. However, a trivial increase in En content, correlated with decreases in Fs and Wo contents, detected in phenocrysts of the porphyritic chondrules, may be meaningful. Chemical composition of high-Ca pyroxene (Table 3) shows only small variations in the range of diopside (B83, B81, B85, B02 and B01) or endiopside (B99 and B84). But, small chemical differences occurring inside separate grains in paired analyses B84–B85, and B81–B83, of high-Ca pyroxene point to a slight but possibly significant chemical heterogeneity within the grains themselves.

OPAQUES

Fe,Ni metal and troilite are the most frequent opaque minerals in the matrix of Baszkówka. Anhedral grains of kamacite, taenite, troilite and accessory chromite, together with their aggregates, complete the inventory of opaque grains in the chondrite (Fig. 10). The origin of opaque grains in ordinary chondrites were outlined over forty years ago, when Urey and Mayeda (1959) recognised them as fragments of a smashed differentiated planet, accreted in secondary parent bodies. Further investigations (Wood, 1967) revealed cooling rates of Fe,Ni metal. The content and distribution of rare elements (Kong and Ebihara, 1996) suggest ordinary chondrite opaques are not nebular condensates, but rather the products of melting and reduction of a material similar to carbonaceous chondrites, in which the chemical composition of metal and sulphide is complementary to the silicate composition of chondrites. However, many genetic details remain doubtful (Brearley and Jones, 1998).

The random distribution of opaques in Baszkówka show some significant exceptions. The most obvious are chains,

Table 10

Fayalite contents in olivine (in wt.%)

Chondrites	Mean	Min.	Max.	Standard deviation
L-type*	–	23.0	25.8	–
Baszkówka	25.9	25.0	27.5	0.83
H-type*	–	26.6	32.4	–

*according to Rubin (1990)

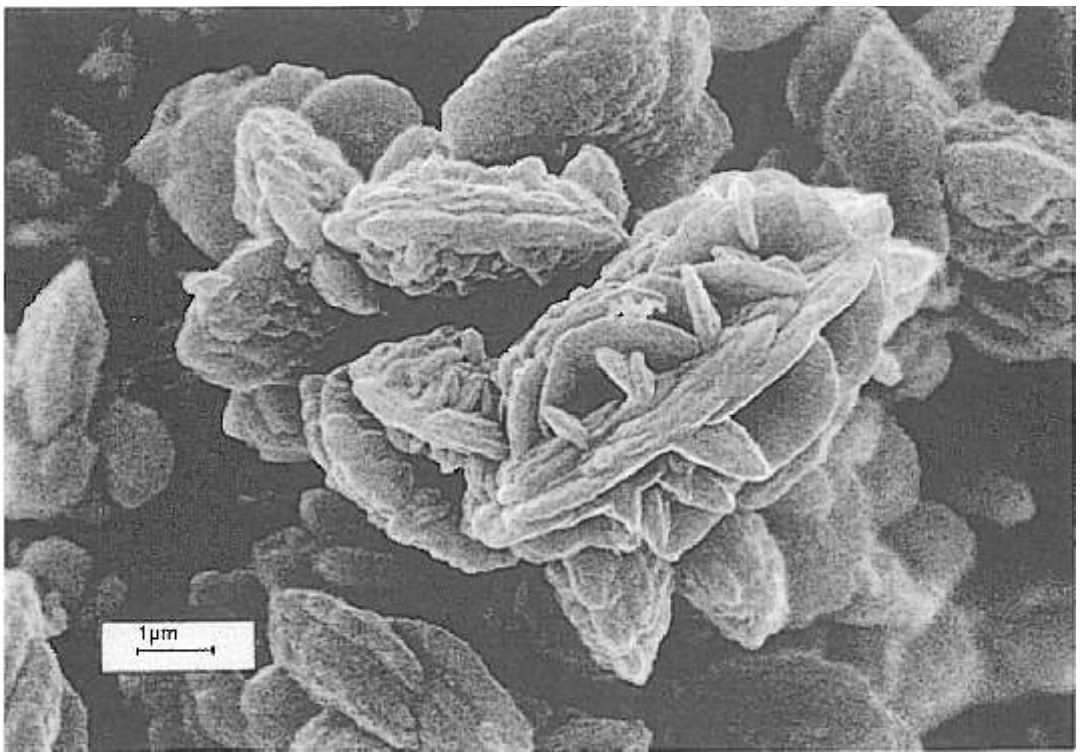

Fig. 25. SEM image; euhedral crystals of copper sulphide (probably idaite) in a fissure within chondrule matrix

from a few millimetres to many centimetres long, mostly of Fe,Ni metal and rarely of troilite grains (Figs. 2 and 3). The origin of such chains remains unclear, although the theory of fluidisation put forward by Huang *et al*. (1996) has found further support. They suggested that this took place in the loose outer regolith of a parent body, where the ascending fluids mobilised Fe, Ni, Co and S carried them in a gas phase. Final recondensation give rise to a rearrangement of Fe,Ni metal and troilite grains (Reisener and Goldstein, 1999), which are mostly ordered in chains (Wasson *et al*., 1996). Certain kamacite particles covered with a troilite shell, rare in chondrites, have analogies in structures created by sulphur mobilisation in a chondritic material (Lauretta *et al*., 1996). Some evidence of fluidisation can be found also in Baszkówka. Namely, a high porosity of the chondrite, intergranular voids (Wlotzka and Otto, 2001) and a deficiency of a fine fraction in the matrix, the latter possibly having been blown off. Moreover, the void walls are covered with tiny crystals with etched faces, the results of intermittent crystallisation from moving, ephemeral fluids. Nevertheless, we consider that the idea of a sedimentary origin for the kamacite (troilite) chains in Baszkówka should not be rejected a priori.

In spite of a high equilibration temperature for the chondrite ~800°C (Wlotzka and Otto, 2001), some important, genetic records endure in structures and textures of Fe,Ni metal as well as troilite-Fe,Ni metal lumps. A particular feature in both kinds of lump, metal and metal-sulphide, are clusters of fissures separating their silicate rims from other components of Baszkówka. Such openings could be a primary effect of accretion of a loose material and/or represent secondary contraction fissures around frozen, shrinking metal or metal-sulphide components of lumps. However, fissures at phase contacts — silicate-metal, silicate-sulphide or metal-sulphide — are small. Moreover, at least in one case (Fig. 17), the composition as well as grain size in the silicate rim are different from that of the surrounding material. In this case, a primary formation for the rim, completed before accretion on the parent body of Baszkówka, is more probable. It is difficult to say, how far similar scenarios could be extrapolated to other particles. Metal-sulphide contacts are smooth, with soft, shallow depressions and swellings, as if both phases were molten, i.e at a temperature over 990°C (Yang *et al*., 1996; Tachibana and Tsuchiyama, 1998). Separation of sulphide from metal melt on a huge scale has taken place inside planetary bodies (Ulff-Moller, 1996; Chabot and Drake, 1999), fragmented in powerful collisions. Discrete drops of metal and sulphide, dispersed in interplanetary space, were combined by random collisions similar to the formation of independent compound chondrules (Wasson *et al*., 1995) relatively soon after planetary collision. A short time later (with metal and sulphide still molten), solid silicate grains were stuck on to the surfaces of molten metal-sulphide drops forming accretion rims. Low-energy collisions deformed the shells of the metal drops, while the original shapes of the more rigid silicates have remained. Deformation of sulphide cores, protected by the metal shells, was less violent. Rapid (high-energy) silicate grains have penetrated deep into the lumps, whereas slow (low-energy) grains simply adhered to the surface. Successive solidification of sulphide and metal occurred in a diminishing temperature range from 990 to 750°C, and the differences of deformability between Fe,Ni metal and troilite resulted in the creation of multiple fractures in FeS cores, disappearing at the contacts of the metal shells.

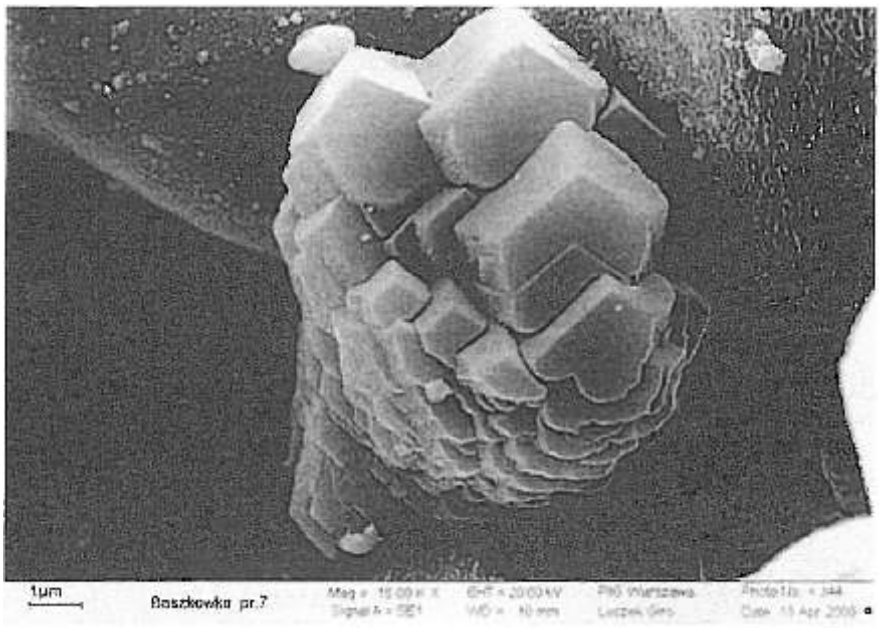

Fig. 26. SEM picture; euhedral crystals of calcite in a fissure within chondrule matrix

FORMATION OF THE BASZKÓWKA PARENT BODY

Slow rotation, asymmetric shapes and a low density (1.5–2.6 g/cm^2) are attributes of asteroids defined at present as rubble piles (Consolmagno and Britt, 1996; Britt and Consolmagno, 1999), that is, loose heaps of planetesimals, having dimensions from a few to a few tens of metres, with numerous void spaces between them. This is a possible concept for the Baszkówka parent body. Its formation and destruction must have been a multistage process (Pilski *et al*., 2001) starting with a collision of molten planetesimals (Sanders, 1996*a*). Low velocity collisions cause "splashing", and much of the resulting spray falls back under the gravity as chondrules (Sanders, 1996*b*), as well as blobs and droplets, possible precursors of metal and/or metal-sulphide lumps from Baszkówka. Meanwhile, the external heating of the Sun (Scott and Rajan, 1981; Kong and Ebihara, 1996), together with internal radioactive heating from ^{26}Al (Hevey and Sanders, 1999), could have produced the thermal metamorphism. Subsequent, low velocity collisions ejected small fragments of planetesimals and provoked gas emission (Wilson *et al*., 1998), mostly of water vapor and carbon dioxide (Huang *et al*., 1996). Violent gas discharges blew off the fine-grained components of shallow regolith horizons, emptying the intergranular spaces between the chondrules, metal-troilite particles, and other medium-grained fragments, and leaving low density, almost matrix-free rock (as in the case of the Baszkówka chondrite). About 70 Ma ago (Wlotzka *et al*., 1997), a moderate collision ejected some fragments of the Baszkówka parent body into interplanetary space, with a shock insufficient to cause any metamorphism in the chondrite: the lowest shock stage S1 (Stöffler *et al*., 1991) has been ascribed to the Baszkówka (Stępniewski *et al*., 1998*a*), whereas most known chondrites show medium stage S3.

CONCLUSIONS

The present results, viewed in terms of the molten planetesimals hypothesis (Sanders, 1996*a*; Pilski *et al*., 2001), suggest:

1. In the beginning, at an early stage of solar nebula development, a glowing mass of dust, gas and molten silicate, metal and sulphide splash-droplets was ejected into space as an effect of violent collisions between molten planetesimals which had already undergone (partial) fractionation. Enormous clouds of incandescent spray cooled in minutes or hours to form chondrules, and over longer time-spans to solidify as large and massive metal or sulphide particles.

2. Collision of molten metal and sulphide droplets molded the compound sulphide core-metal shell droplets in similar manner as inferred for primary-secondary compound chondrules (Wasson *et al*., 1995). The lumps remained molten, while already solidified chondrules or other silicate grains adhered to their surfaces to form their outer rims. More vident impacts of rigid silicate grains on to surfaces of molten metal or metal-sulphide droplets caused the silicate particles to penetrate into the metal and distort its outer surface, whereas the sulphide cores became only slightly deformed.

3. Still molten, or just-solidified lumps and other "clastic" grains landed on temporary accretion surfaces of recreated secondary planetesimals. Most falling particles splashed on to ephemeral accretion surfaces, with only a few, slowly landing particles enduring the shock of impact.

4. Fluids escarping from the Baszkówka parent body blew off fine-grained material from the regolith, making it porous and covering walls of voids with small, euhedral crystals of olivine, pyroxene, plagioclase and other minerals.

5. The internal structure of the Baszkówka parent body, most probably, matched the pattern of a relatively small "rubber pile", and the low-energy impact that launched the Baszkówka fragment into space left no trace of impact metamorphism.

Acknowledgements. The authors are most grateful to E. Starnawska and L. Giro for electron microscopic and microprobe examinations of Baszkówka, and to T. Sztyrak for sample preparation prior to the mineralogical and petrologic studies.

REFERENCES

ALEXANDER C. M. O'. D., PROMBO C. A., SWAN P. D. and WALKER R. M. (1991) — SiC and Si_3N_2 in Qingzhen (EH3). Lunar Planet. Sc. **22**: 5–6.

ALEXANDER C. M. O'. D., SWAN P. D. and PROMBO C. A. (1994) — Occurrence and implication of silicon nitride in enstatite chondrites. Meteoritics, **29**: 79–85.

ANDERSEN C. A., KEIL K. and MASON B. (1964) — Silicon oxynitride, a meteorite mineral. Science, **146**: 256–257.

BORUCKI J. and STĘPNIEWSKI M. (2001) — Two spinel-bearing compound chondrules from the Baszkówka meteorite. Geol. Quart., **45** (3): 281–288.

BREARLEY A. J. and JONES R. H. (1998) — Chondritic meteorites. In: Planetary Materials (ed. J. J. Papike). Rev. Miner., Miner. Soc. America, Washington, D. C., **36** (3).

BRITT D. T. and CONSOLMAGNO G. J. (1996) — Estimation porocities from bulk densities. 59th Annual Meteoritical Society Meeting, July 22–26, 1996, Humbolt-University. Meteor. Planet. Sc., suppl., **31**: A22.

BRITT D. T. and CONSOLMAGNO G. J. (1999) — Asteroid rubble piles: How big are the pieces? (Abstract). 62nd Meteoritical Society Meeting, July 11–16, 1999, Johannesburg. Meteor. Planet. Sc., suppl., **34**: A20.

BUSECK P. R. (1977) — Pallasite meteorites — mineralogy, petrology and geochemistry. Geochim. Cosmochim. Acta, **41** (6): 711–740.

CHABOT N. L. and DRAKE M. J. (1999) — Crystallization of magmatic iron meteorites and liquid immiscibility in the iron-phosphorus-sulfur system. 62th Meteoritical Society Meeting, July 11–16, 1999, Johannesburg. Meteor. Planet. Sc., suppl., **34**: A22–A23.

CONSOLMAGNO G. J. and BRITT D. T. (1996) — Density and porosity measurements of the Vatican meteorite collection. 59th Annual Meteoritical Society Meeting, July 22–26, 1996, Humbolt-University. Meteor. Planet. Sc., suppl., **31**: A31–A32.

CONSOLMAGNO G. J., BRITT D. T. and STOLL C. P. (1998) — Methamorphism, shock and porosity: why are there meteorites? 61th Meteoritical Society Meeting, July 11–16, 1998, Trinity College, Dublin. Meteor. Planet. Sc., **33**: A34–A35.

DYBCZYŃSKI R., DANKO B., KULISA K., POLKOWSKA-MATRENKO H., SAMCZYŃSKI Z., STĘPNIEWSKI M. and SZOPA Z. (1999) — First chemical characterization of the new Polish meteorite "Baszkówka" by neutron activation analysis. Chem. Anal., **44**: 471–484.

HEVEY P. J. and SANDERS I. S. (1999) — Thermal modelling of planetesimals as a constraint on their accretion conditions. 62th Meteoritical Society Meeting, July 11–16, 1999, Johannesburg. Meteor. Planet. Sc., suppl., **34**: A54–A55.

HUANG S., AKRIDGE G. and SEARS D. W. G. (1996) — Metal-silicate fractionation in the suface dust layers of accreting planetesimals: implication for the formation of ordinary chondrites and the nature of asteroid surfaces. J. Geophys. Res., **101** (E12): 29, 373–29, 385.

KEIL K., BERKLEY J. L. and FUCHS L. H. (1982) — Suessite, Fe_3Si: A new mineral in the North Haig ureilite. Am. Miner., **67**: 126–131.

KONG P. and EBIHARA M. (1996) — Metal phases of L chondrites: their formation in the nebula and in the parent body. Geochim. Cosmochim. Acta, **60** (14): 2667–2680.

LAURETTA D. S., LODDERS K. and KREMSER D. T. (1996) — An experimental study of S mobilization during metamorphism of ordinary chondrite parent bodies. 59th Annual Meteoritical Society Meeting, July 22–26, 1996, Humbolt-University. Meteor. Planet. Sc., suppl., **31**: A78.

MANECKI A. (1971) — Cosmic minerals (in Polish with English summary). Prz.Geol., **19** (1): 18–24.

MANECKI A. (1972) — Chondrites and chondrules (in Polish with English summary). Pr. Miner. Komis. Nauk Miner. PAN Kraków, **27**: 7–52.

MARUYAMA S. (2001) — Oxygen-isotopic composition of minerals from Baszkówka chondrite. Geol. Quart., **45** (3): 303–311.

McCOY T. J., EHLMANN A. J. and MOORE C. B. (1997) — The Leedey, Oklahoma, chondrite: fall, petrology, chemistry and an unusual Fe, Ni-FeS inclusion. Meteor. Planet. Sc., **32**: 19–24.

PILSKI A. S., PRZYLIBSKI T. A. and ZAGOŻDŻON P. P. (2001) — Petrology of the chondrite L5 Baszkówka as a reflection of structure and forming process of the parent body surface layer. Meteor. Conf. Olsztyn 26–27 April 2001. Pol. Geol. Inst.: 38–39.

REISENER R. J. and GOLDSTEIN J. I. (1999) — The evolution of metal in chondrites during prograde metamotphism: the role of vapor phase transport. 62th Meteoritical Society Meeting, July 11–16, 1999, Johannesburg. Meteor. Planet. Sc., suppl., **34**: A97–A98.

RIGAKU APPLICATION LABORATORY (1997) — Analysis of a bulk sample of Baszkówka — sample B1, code 10–OXD.

RINGWOOD A. E. (1966) — Chemical evolution of terrestrial planets. Geochim. Cosmochim. Acta, **30**: 41–104.

RUBIN A. E. (1990) — Kamacite and olivine in ordinary chondrites: intergroup and intragroup relationship. Geochim. Cosmochim. Acta, **54** (5): 1217–1232.

RUBIN A. E. (1997) — Mineralogy of meteorite groups. Meteor. Planet. Sc., **32**: 231–247.

SANDERS I. S. (1996*a*) — A chondrule forming scenario involving molten planetesimals. In: Chondrules and the Protoplanetary Disk (eds. R. H. Hewins, R. D. Jones and E. R. D. Scott): 327–334. Cambridge Univ. Press.

SANDERS I. S. (1996*b*) — Significance of acient "impact-melt rocks" for the origin of chondrules. 59th Annual Meteoritical Society Meeting, July 22–26, 1996, Humbolt-University. Meteor. Planet. Sc., suppl., **31**: A122–A123.

SCOTT E. R. D. (1977) — Formation of olivine-metal textures in pallasite meteorites. Geochim. Cosmochim. Acta, **41** (6): 693–710.

SCOTT E. R. D. and RAJAN R. S. (1981) — Metallic minerals, thermal histories and parent bodies some xenolitic, ordinary chondrite meteorites. Geochim. Cosmochim. Acta, **45** (1): 53–67.

SIEMIĄTKOWSKI J. (1998) — Petrografia chondrytu Baszkówka. Pol. Tow. Miner., Pr. Spec., **11**: 160–161.

SIEMIĄTKOWSKI J. (2001) — Petrography of the Baszkówka chondrite. Geol. Quart., **45** (3): 263–280.

STĘPNIEWSKI M., BORUCKI J. and SIEMIĄTKOWSKI J. (1998*a*) — New data on the L5(S1) chondrite Baszkówka (Poland). 61th Meteoritical Society Meeting, July 27–31,1998, Trinity College, Dublin. Meteor. Planet. Sc., suppl., **33** (4): A150–A151.

STĘPNIEWSKI M., SIEMIĄTKOWSKI J., BORUCKI J. and RADLICZ K. (1998*b*) — Fall, recovery and preliminary study of Baszkówka meteorite (Poland). Arch. Miner., **51** (1–2): 131–152.

STĘPNIEWSKI M. and BORUCKI J. (2001) — Pseudometeorite from Łapino (Pomerania, North Poland). Geol. Quart., **45** (3): 343–348.

STÖFFLER D., KEIL K. and SCOTT E. R. D. (1991) — Shock metamorphism of ordinary chondrites. Geochim. Cosmochim. Acta, **55** (12): 3845–3867.

TACHIBANA S. and TSUCHIYAMA A. (1998) — Measurments of evaporation rates of sulfur from iron-iron sulfide melt. 61th Meteoritical Society Meeting, July 27–31, 1998, Trinity College, Dublin. Meteor. Planet. Sc., suppl., **33**: A153.

ULFF-MOLLER F. (1996) — Liquid immiscibility in magmatic iron meteorite parent bodies (Abstract). 59th Annual Meteoritical Society Meeting, July 22–26, 1996, Humbolt-University. Meteor. Planet. Sc., **31**: A144.

UREY H.C. (1952) — The planets. Yale Univ. Press.

UREY H.C. and MAYEDA T. (1959) — The metallic particles of some chondrites. Geochim. Cosmochim. Acta, **17**: 113–124.

Van SCHMUS W. R. and WOOD J. D. (1967) — A chemical-petrologic classification for the chondritic meteorites. Geochim. Cosmochim. Acta, **31** (5): 747–765

WASSON J. T. and WAI C. M. (1970) — Composition of the metal, schreibersite and perryite of enstatite achondrites and the origin of enstatite chondrites and achondrites. Geochim. Cosmochim. Acta, **34**: 169–184.

WASSON J. T., KROT A. N., LEE M. S. and RUBIN A. E. (1995) — Compound chondrules. Geochim. Cosmochim. Acta, **59** (9): 1847–1869.

WASSON J. T., ZITO K. L. and ULFF-MOLLER F. (1996) — Matrix composition and flow in ordinary chondrites. 59th Annual Meteoritical Society Meeting, July 22–26, 1996, Humbolt-University. Meteor. Planet. Sc., **31**: A147.

WEINBRUCH S., BÜTTNER H., ROSENHAUER M. and HEWINS R. H. (1996) — On the lower limit of chondrules cooling rates. 59th Annual Meteoritical Society Meeting, July 22–26, 1996, Humbolt-University. Meteor. Planet. Sc., **31**: A149–150.

WILSON L., KEIL K. and LOVE S. G. (1998) — Factors controlling the bulk densities of asteroids. 61th Meteoritical Society Meeting, July 27–31,1998, Trinity College, Dublin. Meteor. Planet. Sc., **33**: A168.

WLOTZKA F. (1995) — Baszkówka. In: Catalogues and Inventories. Meteor. Bull., **78**, Meteoritics, **30**: 792–796.

WLOTZKA F. and OTTO J. (2001) — Euhedral crystals in interstitial pores of the Baszkówka and Mt. Tazerzait L5 chondrites. Geol. Quart., **45** (3): 257–262.

WLOTZKA F., SCHERER P., SCHULTZ L., OTTO J. and STĘPNIEWSKI M. (1997) — Petrography and noble gases of the unusual L5 chondrites Baszkówka and Mt. Tazerzait. Meteor. Planet. Sc., suppl., **32** (4): A140–A141.

WOOD J. A. (1967) — Chondrites: Their metallic minerals, thermal histories, and parents planets. Icarus, **6**: 1–49.

YANG C. -W., WILLIAMS D. B. and GOLDSTEIN J. I. (1996) — Taenite decomposition in meteoritic metal at low temperatures (<400°C). 59th Annual Meteoritical Society Meeting, July 22–26, 1996. Humbolt-University. Meteor. Planet. Sc., suppl., **31**: A156–A157.